The Diffuse Interstellar Medium

Robin Shelton

Structure

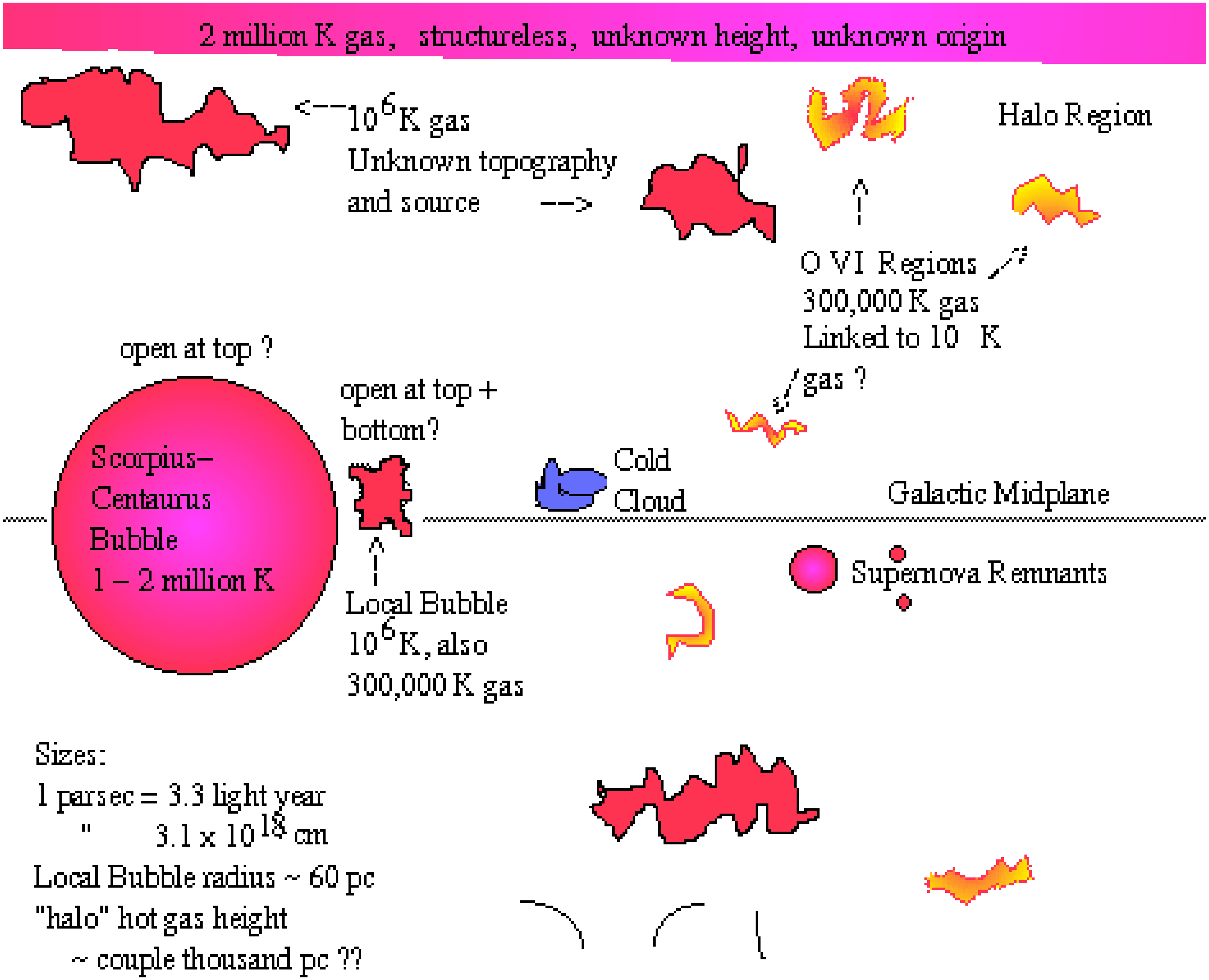
2 million K gas, structureless, unknown height, unknown origin
<--10^6K gas
Unknown topography
and source -->
Halo Region
O VI Regions
300,000 K gas
Linked to 10 K
gas ?
open at top ?
Scorpius-
Centaurus
Bubble
1 – 2 million K
open at top +
bottom?
Cold
Cloud
Galactic Midplane
Supernova Remnants
Local Bubble
10^6K, also
300,000 K gas
Sizes:
1 parsec = 3.3 light year
" 3.1 x 10^{18} cm
Local Bubble radius ~ 60 pc
"halo" hot gas height
~ couple thousand pc ??

Outline

- Large bubbles
  - Local Bubble -- Spoiler: Solar Wind Charge Exchange
  - Sco-Cen Bubble (Loop I)
- Supernova Remnants (see later talks)
- Galactic halo
- Galactic Ridge and Bulge (see later talks)

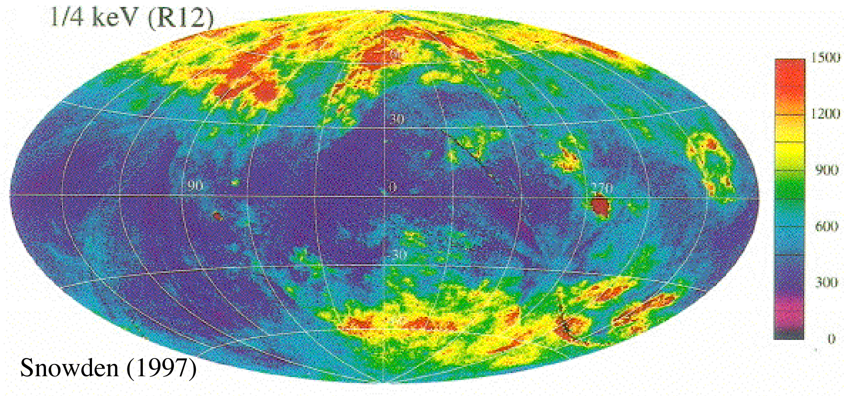

Snowden (1997)

Fig. 2. Smoothed galactic $N_{H\,I}$ image of the cloud (velocity interval: -30 km s^{-1} < $V_{H\,I}$ < -17 km s^{-1}). The field is the same as for Fig. 1; the minimum contour is 0.5×10^{20} H I cm^{-2} with contour intervals of 0.5×10^{20} H I cm^{-2}.

Snowden et al. (1991)

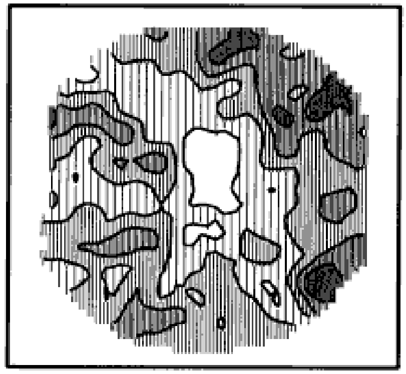

Fig. 1. Smoothed x-ray image of the shadow. The minimum contour is at 6×10^{-4} count s^{-1} arc min^{-2} with contour intervals of 2×10^{-4} count s^{-1} arc min^{-2}. The field is 1.8° in diameter with the center at $\ell \sim 94.7°$, $b \sim -37.6°$; longitude increases to the left and the north galactic pole is up.

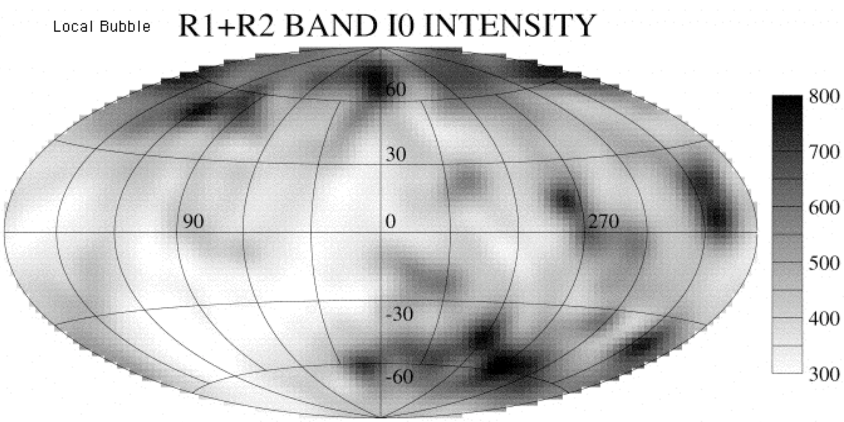

Snowden et al. (1998)

Historical View of Local Bubble:

- Soft X-rays observed from all directions, anti-correlated with N_H, hence Local Bubble (LB) (Wisconsin All Sky Survey, SAS 3, HEAO 1, ROSAT, also XMM, Chandra, Suzaku)
- ROSAT images reveal shadows, confirms local X-ray emission
- LB stronger in 1/4 keV than 3/4 keV (ex: ratio > 15, Snowden, McCammon, & Verter (1993) in MBM 12 direction)
- LB mapped via shadowing analyses (Snowden et al. 1998, Kuntz & Snowden 2000),
- Temperature: if CIE, then $T \sim 10^6$ K, $P \sim 15{,}000$ K/cm^3
- Radius: 50 to 120 pc, depending on direction (Snowden et al. 1998)

But, Solar Activity Also Makes Local Diffuse X-Rays

- Solar wind ions charge exchange with neutral gas (ex: O^{7+} + H or He -> O^{6+*} + H^+ or He^+), then de-excite and radiate X-ray photons ∴ contaminate observations
- Solar activity level is cyclic
- The ROSAT All Sky Survey and the XMM and Chandra LB observations were taken during solar maximum
- Present time = solar minimum, thus current Suzaku observations see minimal solar effects

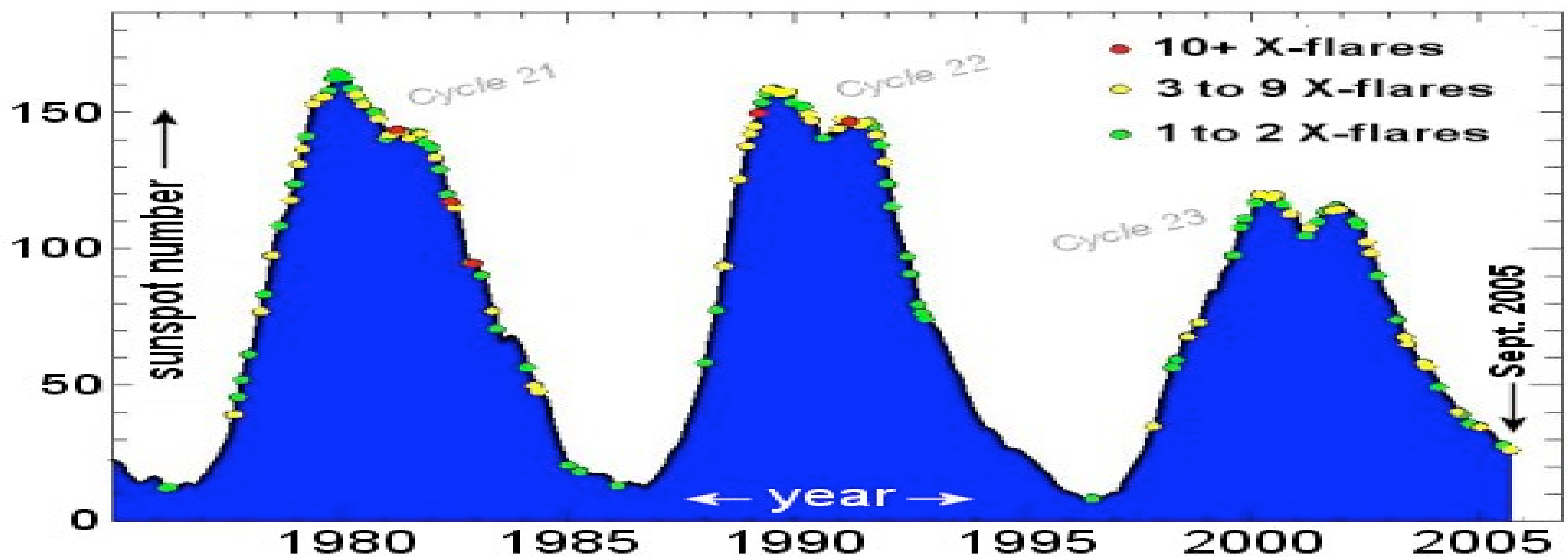

Solar Wind Charge Exchange (SWCX) Spectrum

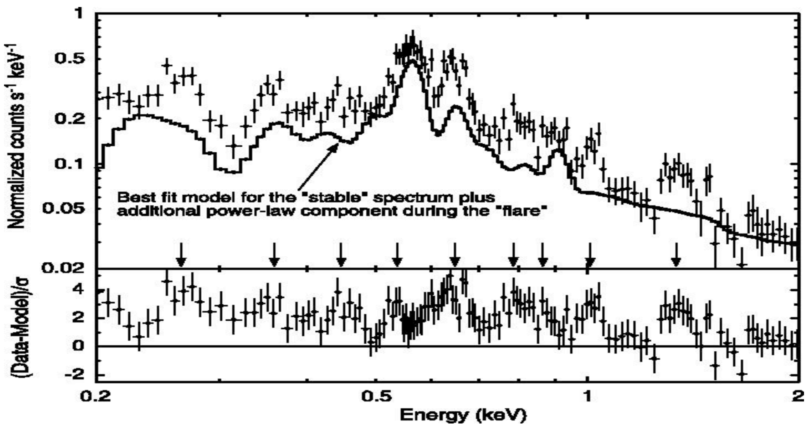

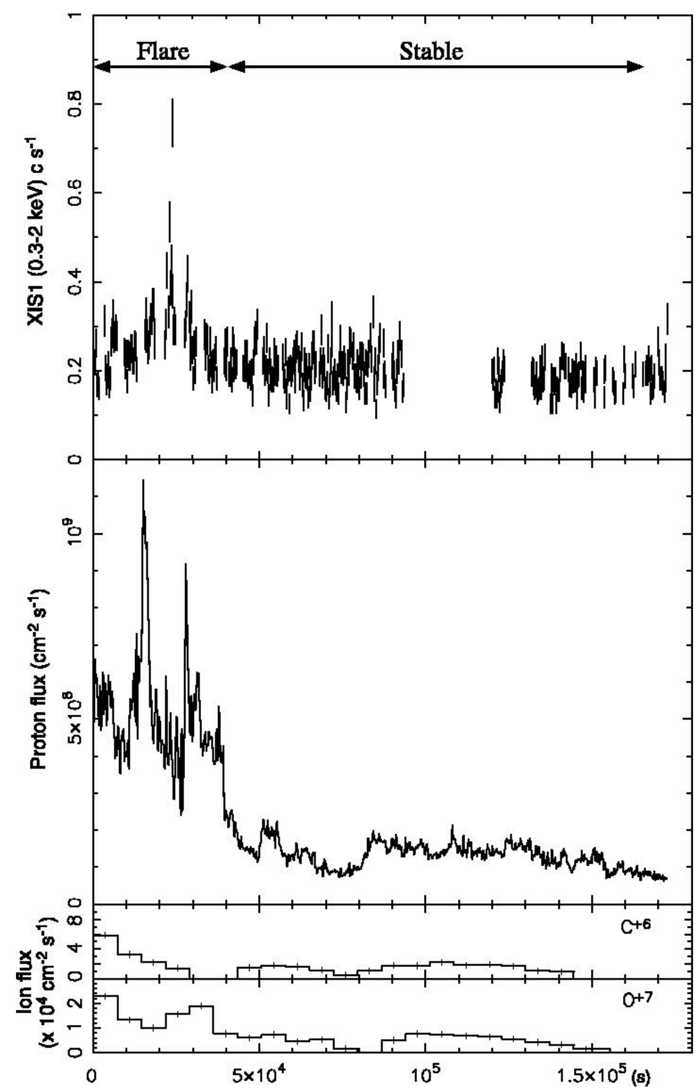

- Suzaku Spectrum (Fujimoto, et al. 2007)
  - 357 eV: C VI 2p to 1s
  - 455 eV: C VI 4p to 1s
  - 558 eV: O VII (561 eV)
  - 649 eV: O VIII (2p to 1s (653 eV)
  - 796 eV: Fe XVII, XVIII L and O VIII 3p to 1s
  - 882 eV: Fe XVII, XVIII L + Ne IX + O VIII 6p to 1s
  - 1022 eV: Ne X
  - 1356 eV: Mg XI
- SWCXflare correlated with ACE observations of proton flux
- Emission thought to be geocoronal

Another type of SWCX Event

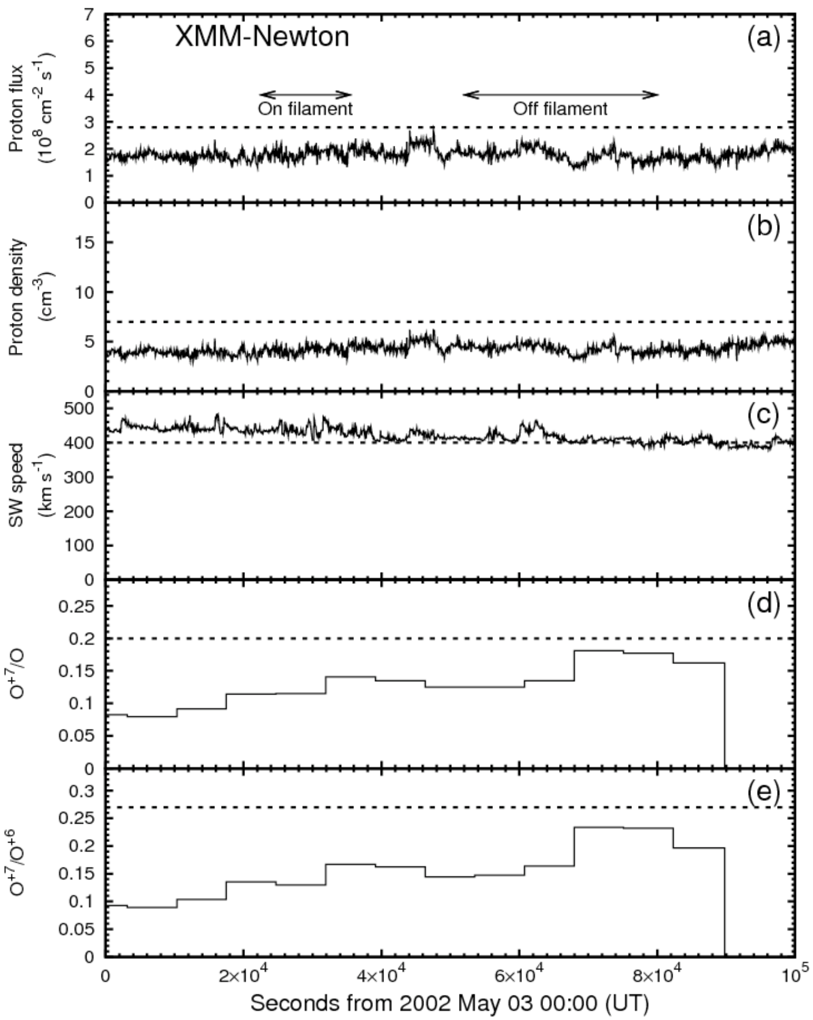

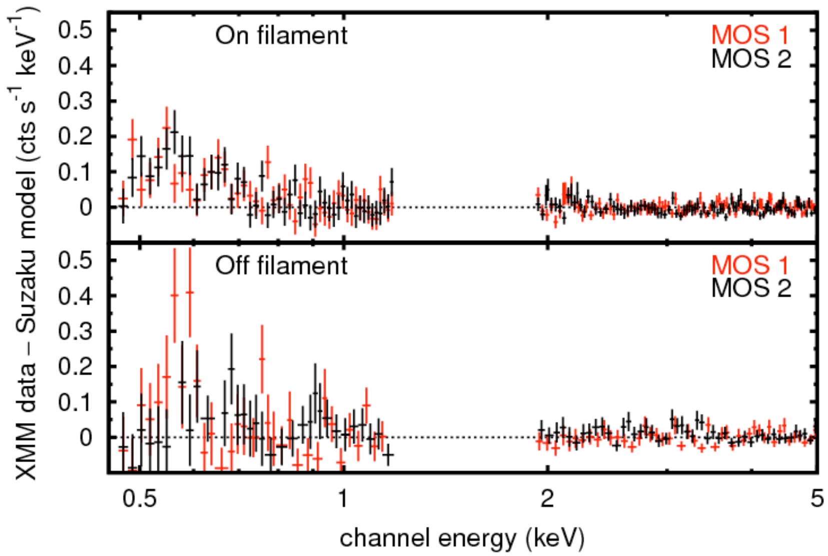

- XMM and Suzaku observed same directions 4 years apart
- ACE showed no anomalies during the XMM observation, but XMM saw much more X-ray emission than Suzaku (Henley & Shelton, 2007)
- ∴SWCX can be uncorrelated with ACE diagnostics => <u>heliospheric</u> "density enhancements"

Density Enhancements - Coronal Mass Ejections

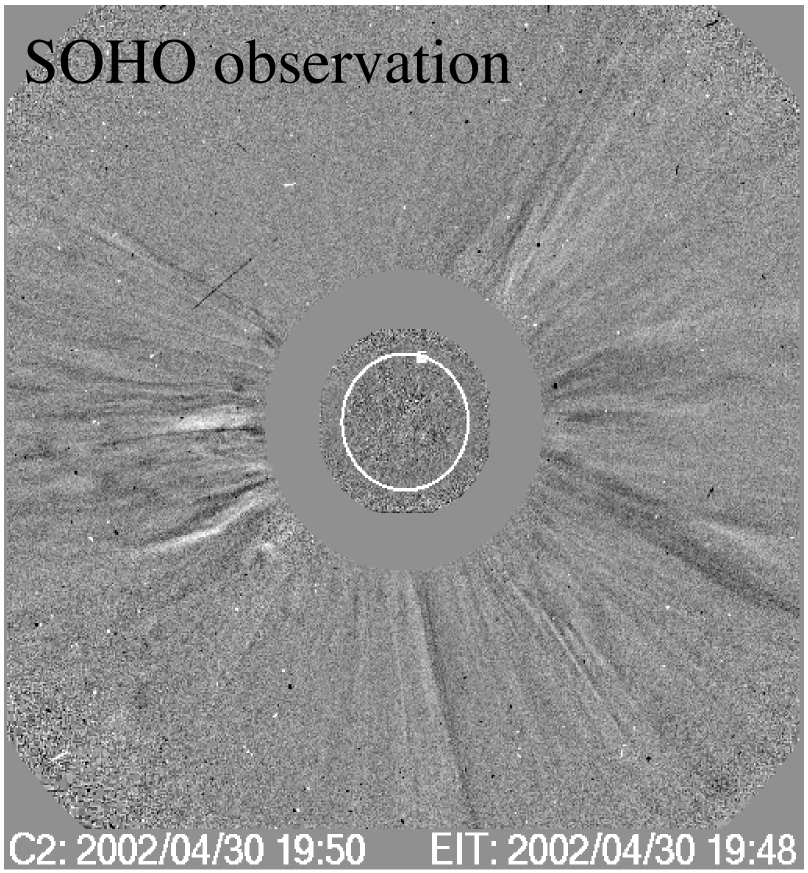

- Cause:
  - perhaps density enhancements (Coronal Mass Ejections) that create X-rays but need not intersect ACE satellite
  - Coronal Mass Ejections (Koutroumpa, et al. 2007)
- Thus, there can be non-quiescent <u>heliospheric</u> SWCX, too
- How much? XMM event

  O VII: 4 to 7 ph/s/cm^2/sr

  O VIII: 1 to 5 ph/s/cm^2/sr

Also Steady Heliospheric SWCX

- Robertson, Cravens & Snowden (2003), Koutroumpa, et al. (2007), and Henley & Shelton (2007) calculated steady heliospheric SWCX
- Directional dependence assoc. with activity on Sun's surface

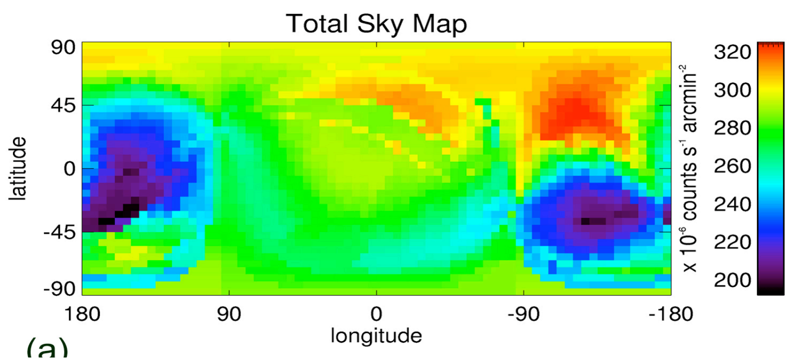

Robertson, Cravens, and Snowden (2003) Predictions for SWCX seen by ROSAT All Sky Survey

How Can We Make Progress on SWCX?

Geocoronal:
Fujimoto et al

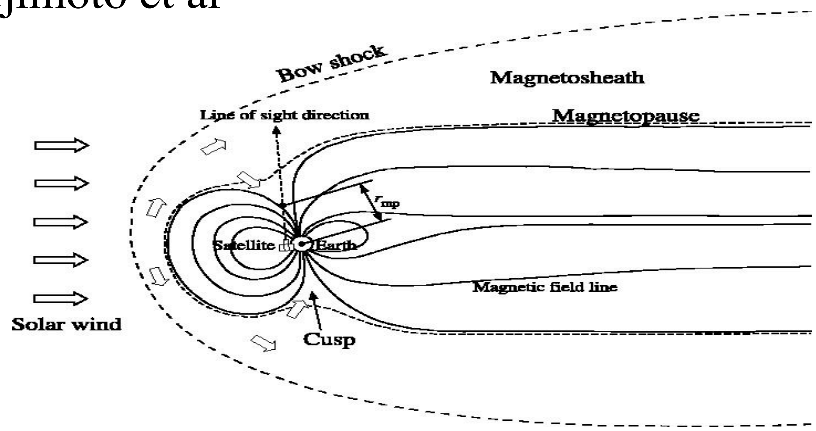

Heliospheric:
Robertson & Cravens

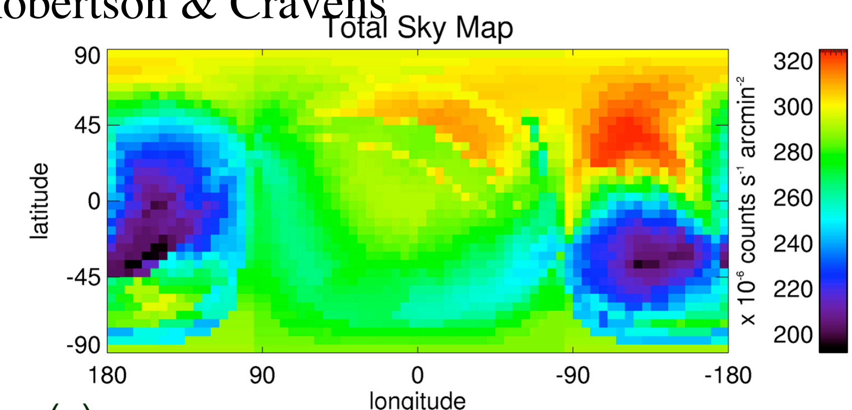

(a)

- Active area! See 3 posters
- Observations: examine geocoronal vs heliospheric vs Coronal Mass Ejection SWCX
- Continue work on theoretical SWCX estimates
  - improved atomic physics in the 1/4 keV band
  - uncertainty estimates
  - spectral temperature of the SWCX

SWCX Does Not Negate the Local Bubble

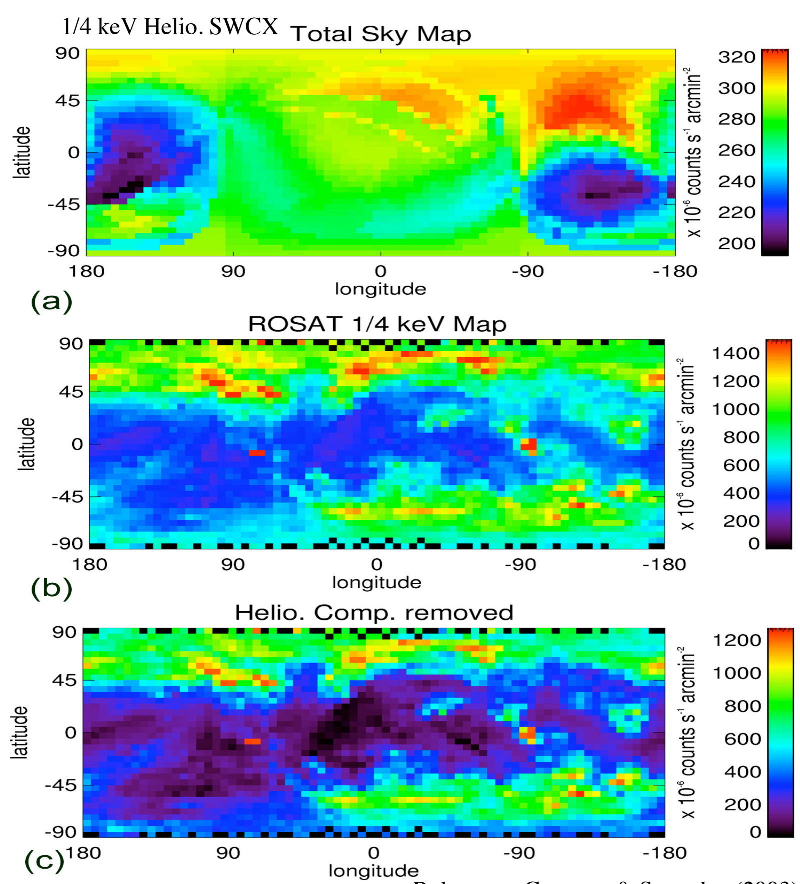

Robertson, Cravens, & Snowden (2003)

- 1/4 keV: Robertson & Cravens (2003) model explains ~50% of 1/4 keV emission found in Gal. plane and ~25% of emission at high latitudes
- Significant 1/4 keV emission remains after SWCX subtraction
- Other reasons to believe in LB:
  - O VI column density cannot be explained by SWCX
  - A cavity in the cool gas distribution surrounds the Solar neighborhood; the space must be filled by some phase of the ISM

Local Bubble Observations

•Use shadowing technique to distinguish Local Bubble from Galactic halo

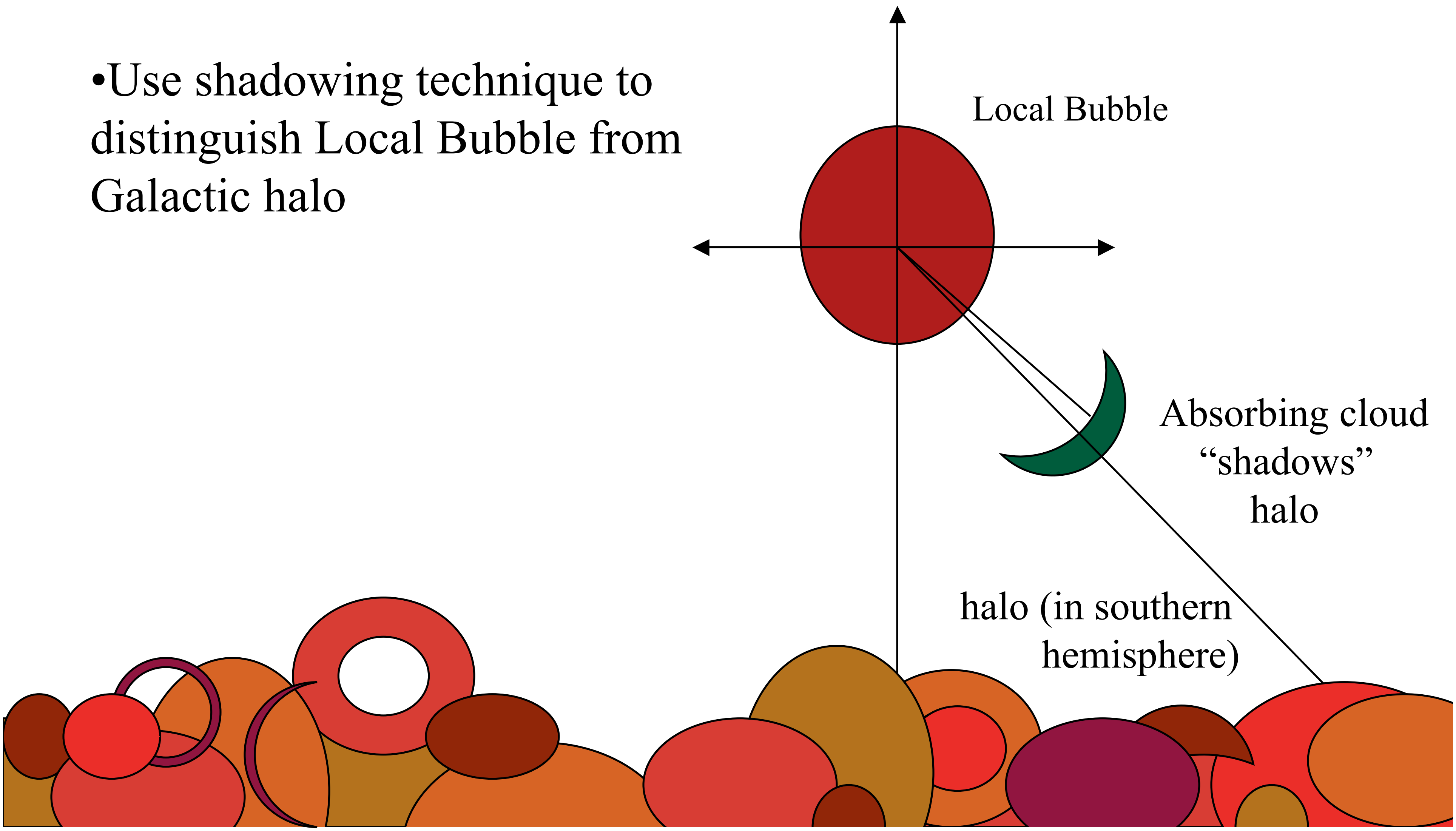

Suzaku Shadowing Observations of the Local Bubble

- Suzaku => taken solar minimum observations
- MBM 12 (Smith et al. 2007)

  O VII: 3.34 ± 0.26 l.u. - 3.5 l.u. (SWCX, Koutroumpa)

  O VIII: 0.24 ± 0.1 l.u. - 0.5 l.u. (SWCX, Koutroumpa)
- Southern filament (Henley & Shelton 2007)

  $\mathrm{Log}(T_{LB}) = 5.98(+0.03,-0.04)$

  O VII: 1.1(+1.1,-1.4) l.u. - 0.8 l.u. (SWCX, Koutroumpa)

  O VIII: 1.1 ± 1.1 l.u. - 0.1 l.u. (SWCX, Koutroumpa)

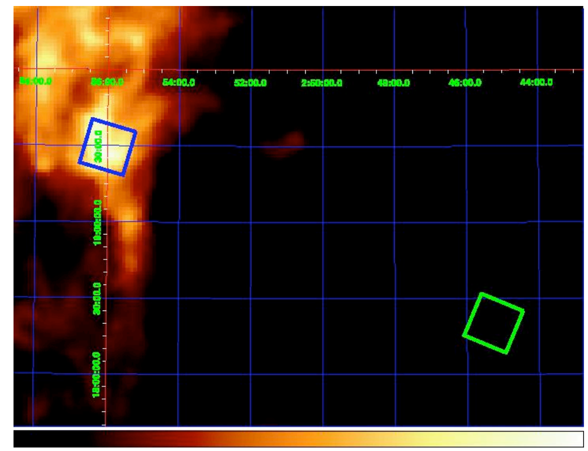

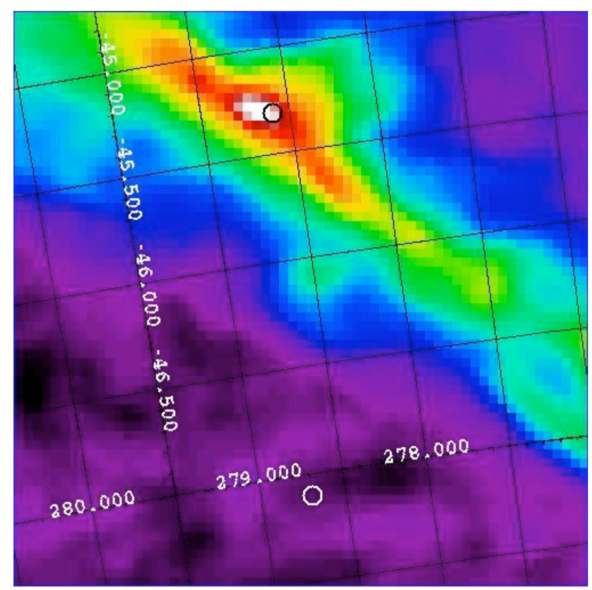

Another Large Bubble: Loop I, North Polar Spur

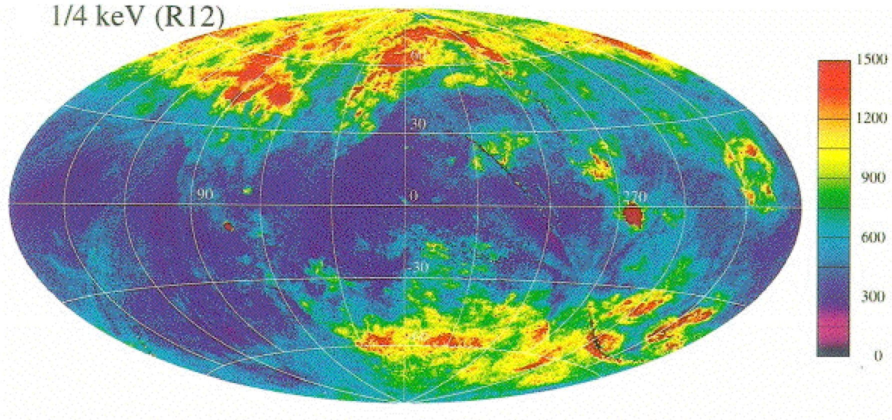

- Suzaku observation (Miller et al. 2007)
- Unusual metal abundances, elevated nitrogen
  - Suggests region was enriched by AGB stars
  - Enrichment is not related to bubble, because AGB stars are too old

Hot Gas in the Halo / Thick Disk

- Height = above disk H I layer
  - shadows distinguish LB from halo
- Turn of the century picture:
  - "halo" emits 1/4 keV and 3/4 keV X-rays
  - 2 T model (1 and 3×10^6 K), Kuntz & Snowden (2001)
  - ROSAT maps show 1/4 keV distribution is lumpy, but 3/4 keV emission is smooth (aside from Loop I) so expect 2 components

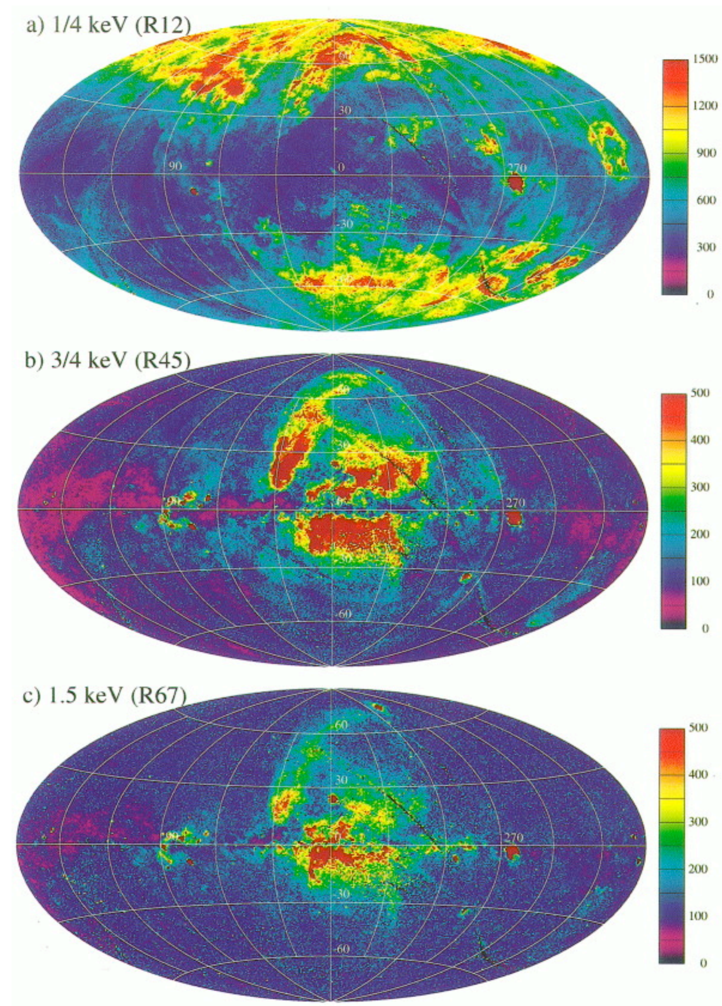

Chandra, XMM, Suzaku Era

Yao & Wang, 2007, Chandra

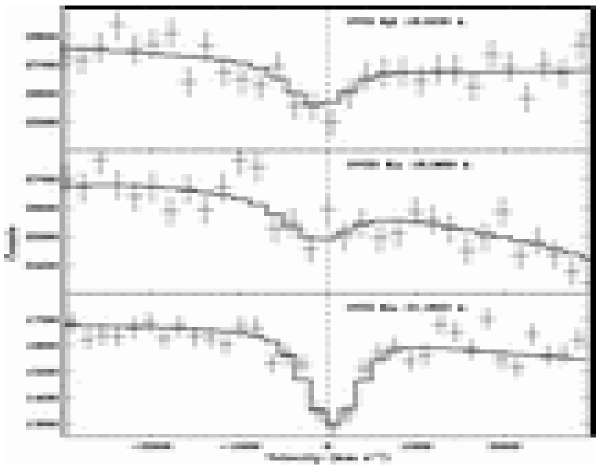

Lei, et al. in prep

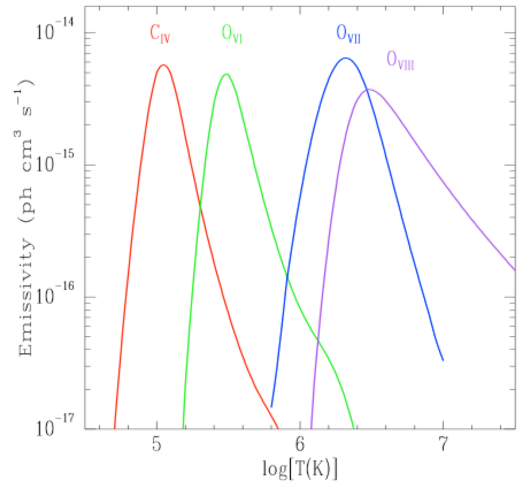

- Observe O VII and O VIII features, spectra
- Combine with C IV and O VI data to span wider temperature range
- Consider new models:
  - non-equilibrium
    (have not found significant signs of disequilibrium)
  - non-isothermal

Power Law Emission Measure Models

- $d(n_e^2 dl)/d(\log T) \propto T^{\alpha}$

- 2 versions

  First version:

  - Yao & Wang (2007)
  - modeled O VI (abs), O VII & O VIII (abs + emiss) together
  - Mrk 421 and $l \sim 90°$, $b \sim 61°$
  - Found $\alpha = 1.2$

Power Law Emission Measure Models

- $d(n_e^2 dl)/d(\log T) \propto T^{\alpha}$ continued
- second version:
  - Lei, Shelton, & Henley (in preparation),
  - used O VI (abs & emiss), ROSAT 1/4 keV, and Suzaku spectrum (covered O VII & O VIII)
  - Southern Filament shadowing analysis (l = 279°, b=-47°)
  - Required 2 components
  - Found $\alpha_1 = 0.4$, and $\alpha_2 = -2$
  - Explains differing 1/4 keV and 3/4 keV distributions

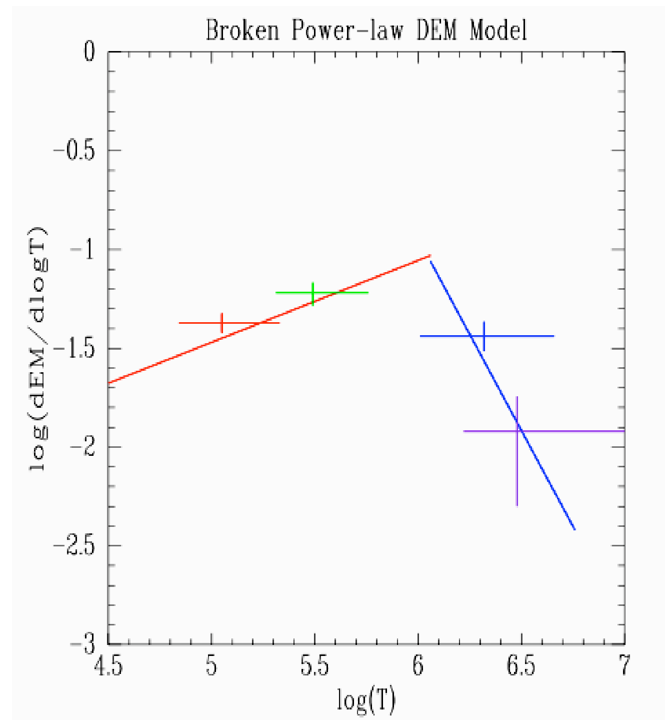

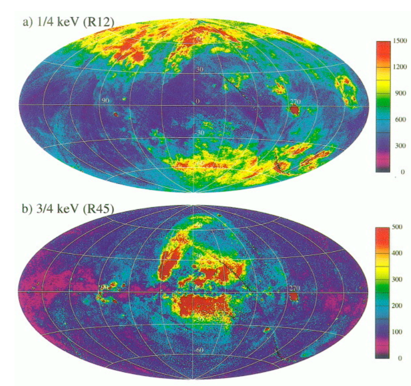

Conclusions

- Solar wind charge exchange X-rays observed:
  - Some flairs are correlated with ACE proton flux
  - Some flairs are not (maybe line of sight enhancements)
  - Complicate observations of the Local Bubble but do not negate the Local Bubble
- Local Bubble observations: Temperature near previous estimate, O VII and O VIII measured
- North Polar Spur observations: generally agree with previous results, but find enhanced nitrogen
- Halo: replaced 1 and 2 T models with power law models. Source of 3/4 keV emission differs from source of 1/4 keV emission

Supplemental

FUSE Shadowing Observations

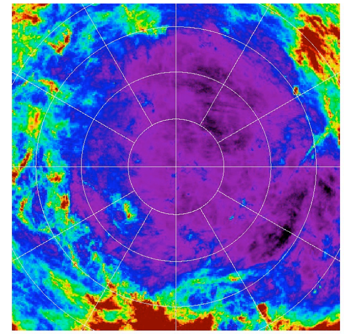

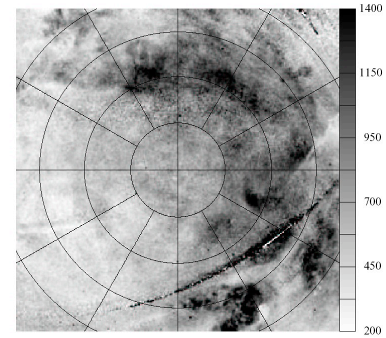

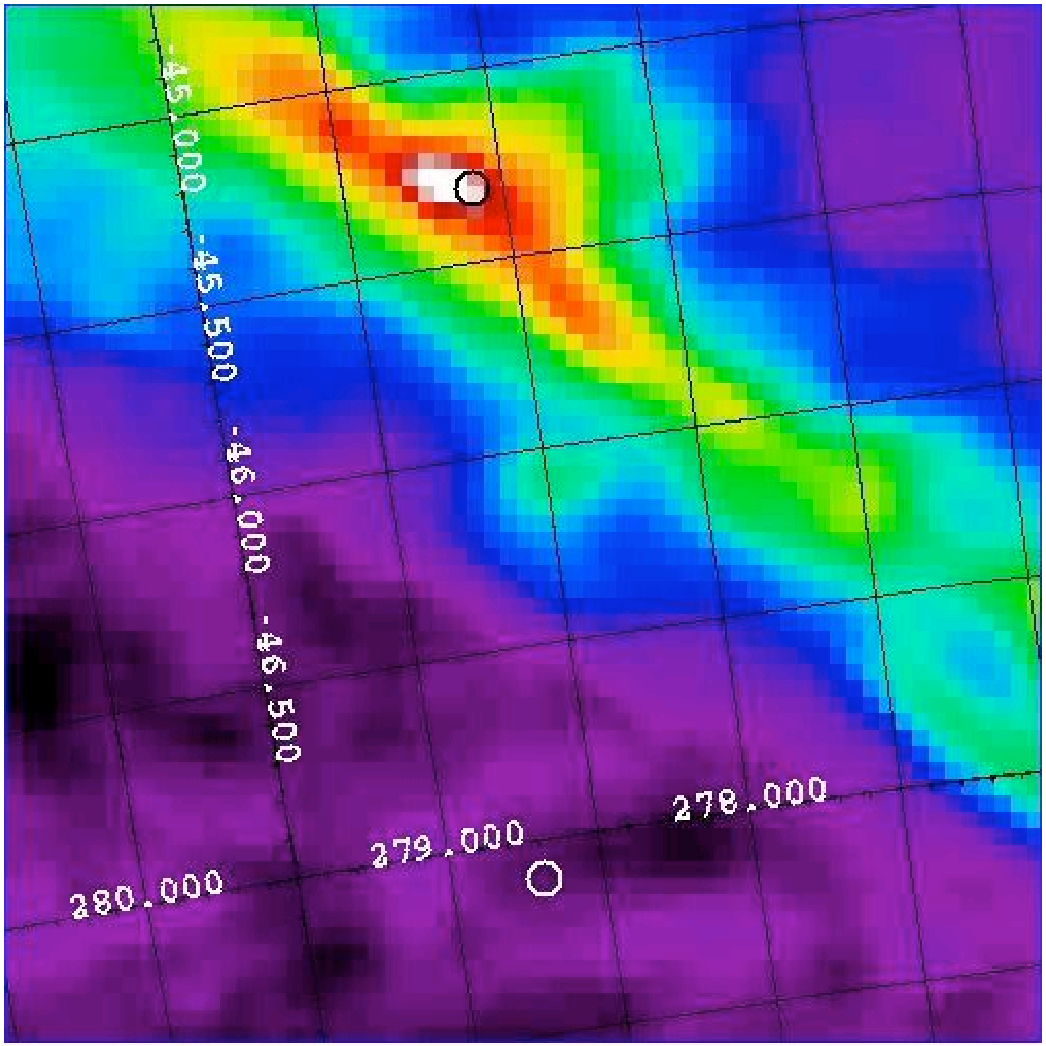

- Not unusual part of southern halo
- On-filament:

  l = 278.6, b = -45.3

  E(B-V) = 0.17 ± 0.5 magnitudes

  (Penprase et al. 1998)

  IRAS 100 μm => 7.3 MJy sr^{-1}

  (Schlegel et al 1998)

  Filament blocks 89 (+5,-11)%

  of 1032, 1038 Å photons
- Off-filament:

  l = 278.7, b = -47.1

  N_H = 0.5 to 2.0 × 10^{20} cm^{-2}

  (Lallement et al. 2003, Kalberla et al. 2005, Schlegel et al. 1998)

  Transmits 59% to 88%

  of 1032, 1038 Å photons

Halo's Emission Measure Function

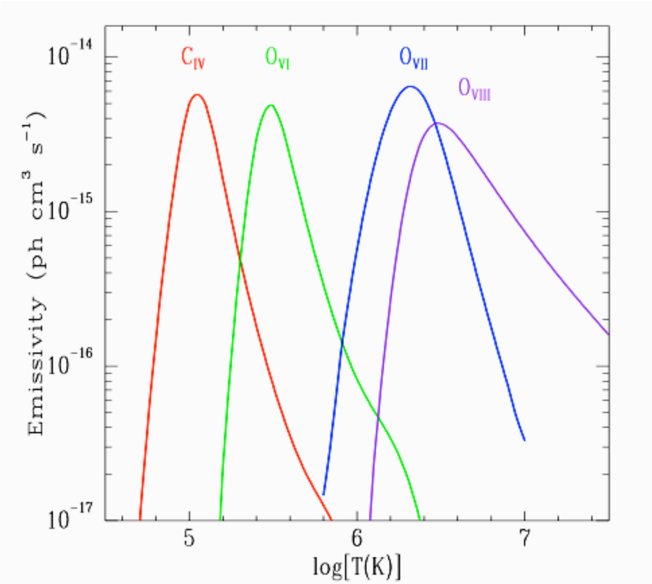

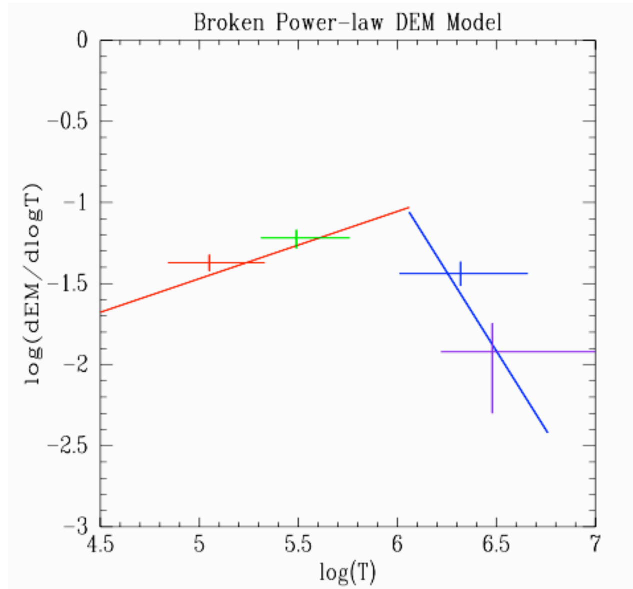

- Tracers over broad range of temperatures

  10^5 K: C IV (SPEAR)

  3×10^5 K: O VI (FUSE)

  2×10^6 K, 3×10^6 K: O VII and O VIII (Suzaku, XMM, Chandra)
- Spectral Fitting
- Power laws explain obs better than 1 or 2 temperature models
  - Yao & Wang (2007), toward Mrk 421 (Chandra)

    Lei, Shelton, & Henley (in preparation), near Southern Filament (Suzaku)

How Can We Make Progress, continued

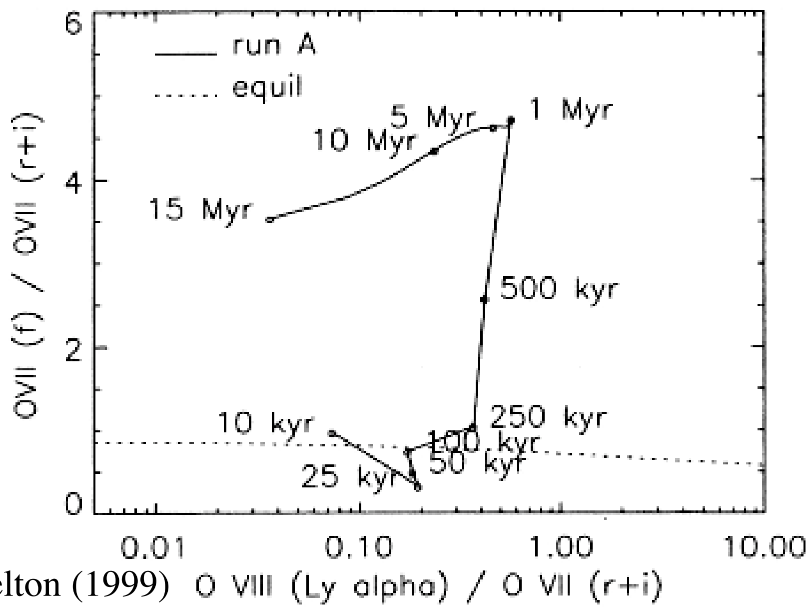

Shelton (1999)

- Test for SWCX; Search for clever solar system observing strategies
- Pursue high spectral resolution observations, but with note that spectral signature of recombining SW could look similar to recombining gas in the LB
  - Ex: O VII forbidden to recombination + intercombination ratio

History: Local Cavity

- Na I data implies cavity in neutral material
- Size: r ~ 65 to ~250pc
- Note possible chimney
- Early hints: β CMa Tunnel - Gry et al. 1985,
- Recent surveys: Welsh et al, 1998, Sfeir et al. 1999, Lallement at al. 2003

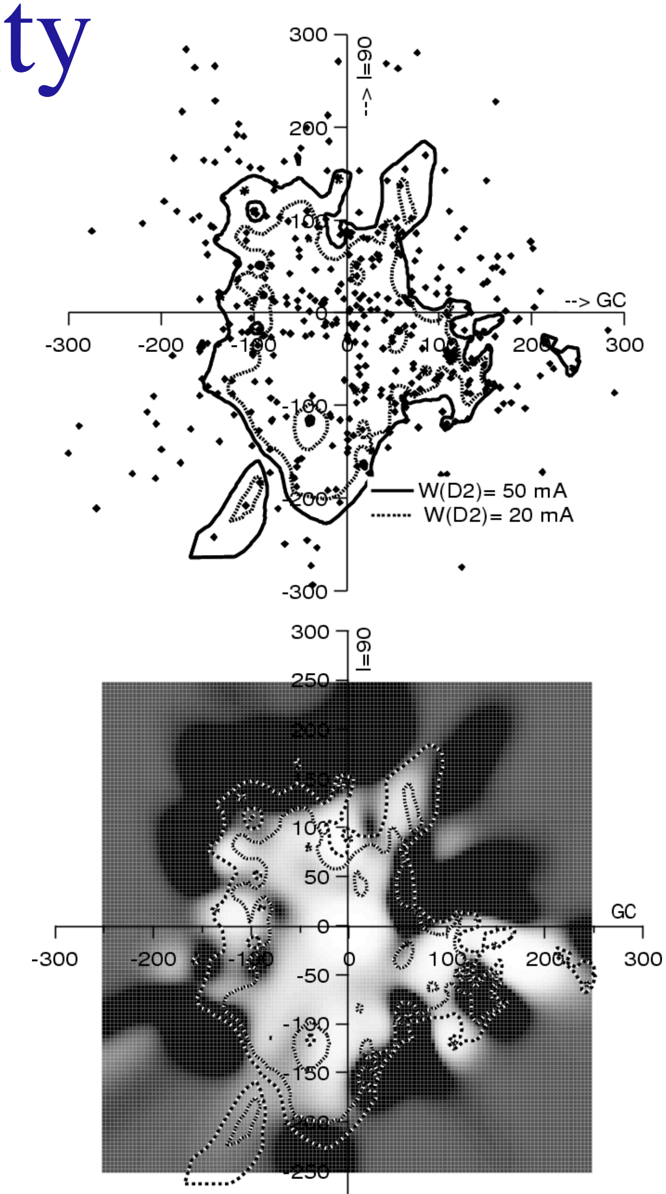

Lallement et al. (2003)

History: O VI

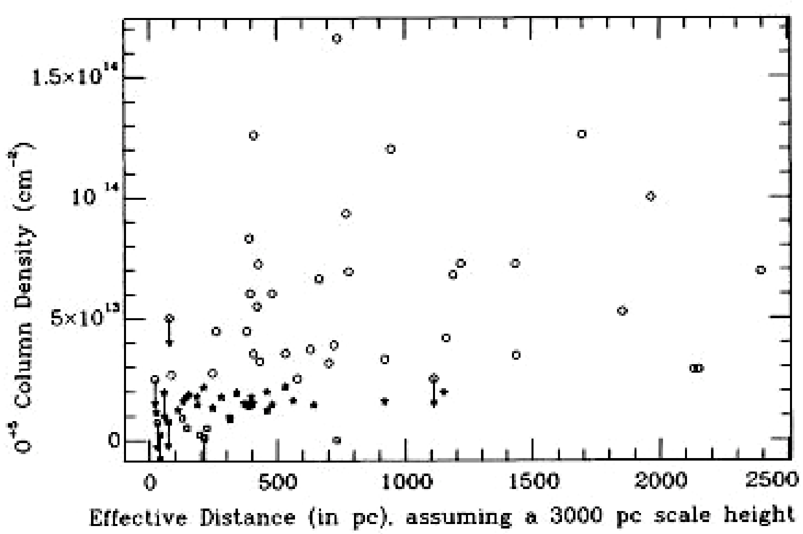

FIG. 3.—Same as Fig. 2 but with a 3000 pc scale height
Shelton & Cox (1994) from Jenkins (1978)

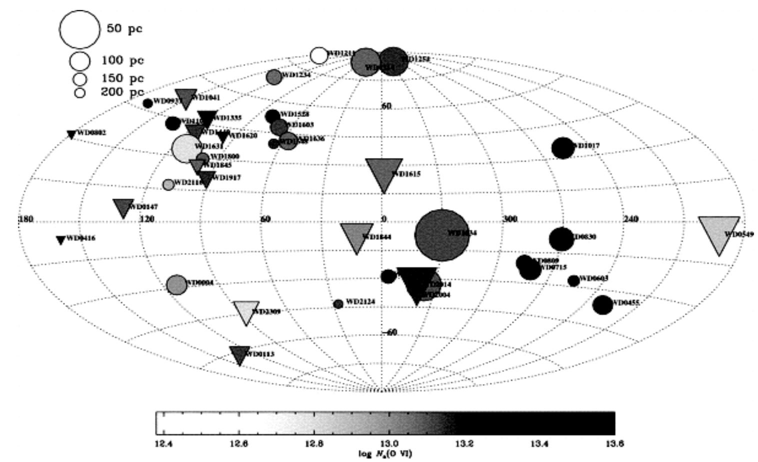

Savage & Lehner (2006), O VI observations

- O VI found in *Copernicus* survey
  - O VI column density found on nearby sightlines (Jenkins 1978)
  - Offset in straight line fit to column density vs distance data (“)
  - Statistical analysis found O VI in LB to be probable ($N_{OVI} \sim 1.6 \times 10^{13}$ cm^{-2}, Shelton & Cox 1994)
- O VI column density found in *FUSE* surveys of nearby stars
  - Oegerle et al. 2005 ($N_{OVI} \sim 0.7 \times 10^{13}$ cm^{-2} per 100 pc)
  - Savage & Lehner 2006 ($N_{OVI} \sim 1.1 \times 10^{13}$ cm^{-2} per 100 pc, local n_{OVI} is higher than disk average)

History: Suggestion that the LB isn't Hot

- Re-examine CIE assumption
- Ex: hot gas bubble "breaks out" of birth cloud
  - Rapidly adiabatically expands
  - Gas cools faster than ions recombine
  - Very high ions -> X-rays
  - Fig: Breitschwerdt 2001

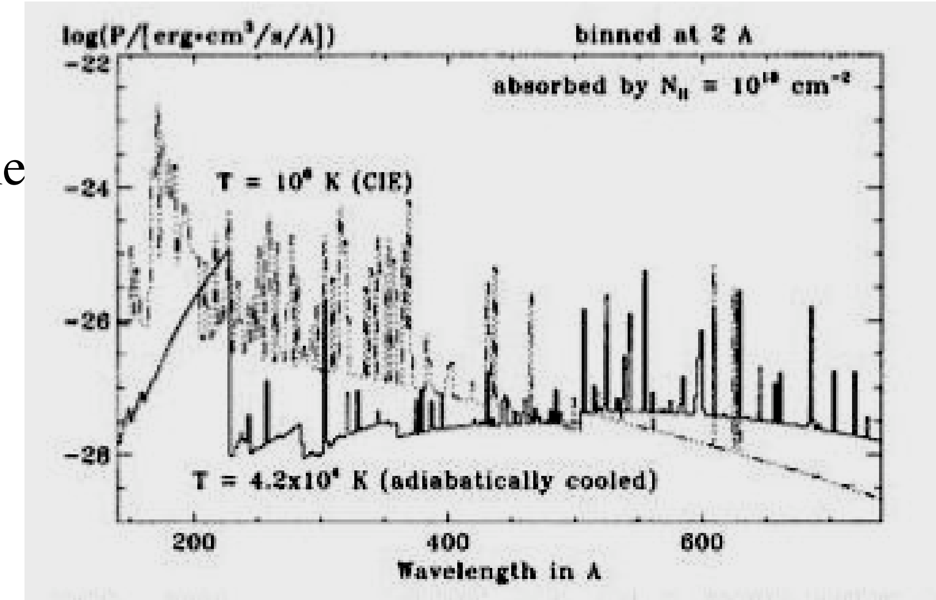

- Expect O VI within LB
  - $N_{OVI} \approx 2.7 \times 10^{14}/cm^2$
  - $I_{OVI} \approx 1900$ ph/s/cm^2/sr
  - (My estimates from Breitschwerdt model)

History: Simulations

- Single SNRs simulated, but provided too little energy to explain 1/4 keV
- Multiple SNRs simulated
  - Our region of Galaxy, assuming realistic IMF. The Local Bubble after 20 SN have exploded ➡ (fig: Avillez 2003)
  - Non CIE simulations of bubble blown by 2 to 3 SN
    - $N_{OVI} = 0.8 - 2.8 \times 10^{13}/cm^2$ (corrected)
    - I_{OVII}, I_{OVIII} = few to several $ph/s/cm^2/sr$
    - (ref: Smith & Cox 2001)

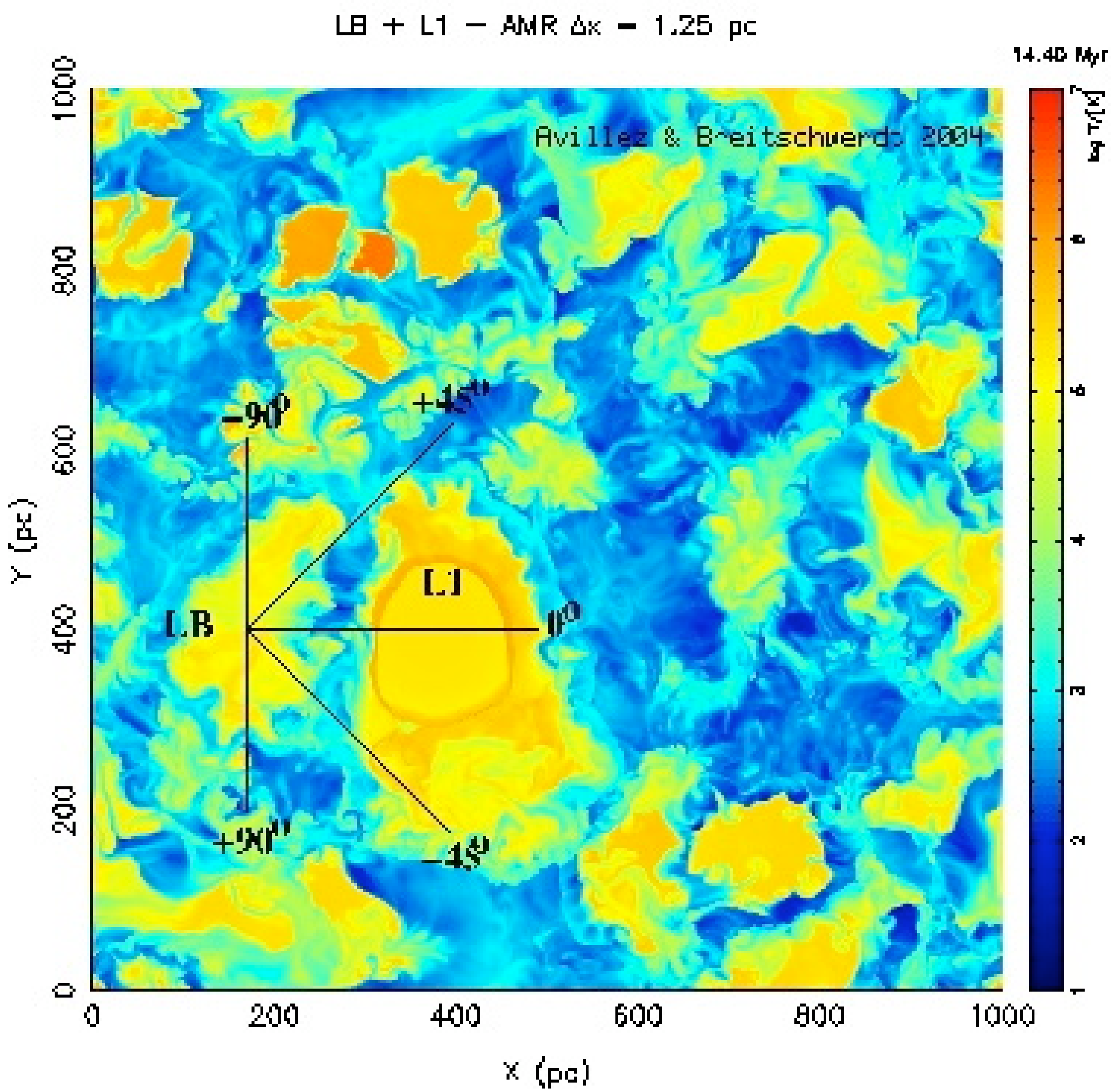

History: Multiple SNR explanation

- Sco-Cen stars or Pleiades stars may have passed through solar neighborhood within last 10 to 20 million years
- Expect 10 to 20 early SN
- Blow Local Bubble, and shower Earth with cosmic rays and ^{60}Fe
- ∴ extinctions and observed ^{60}Fe layers
- (Fig: Maiz-Apellaniz 2001, Also see Berghofer & Breitschwerdt 2002)

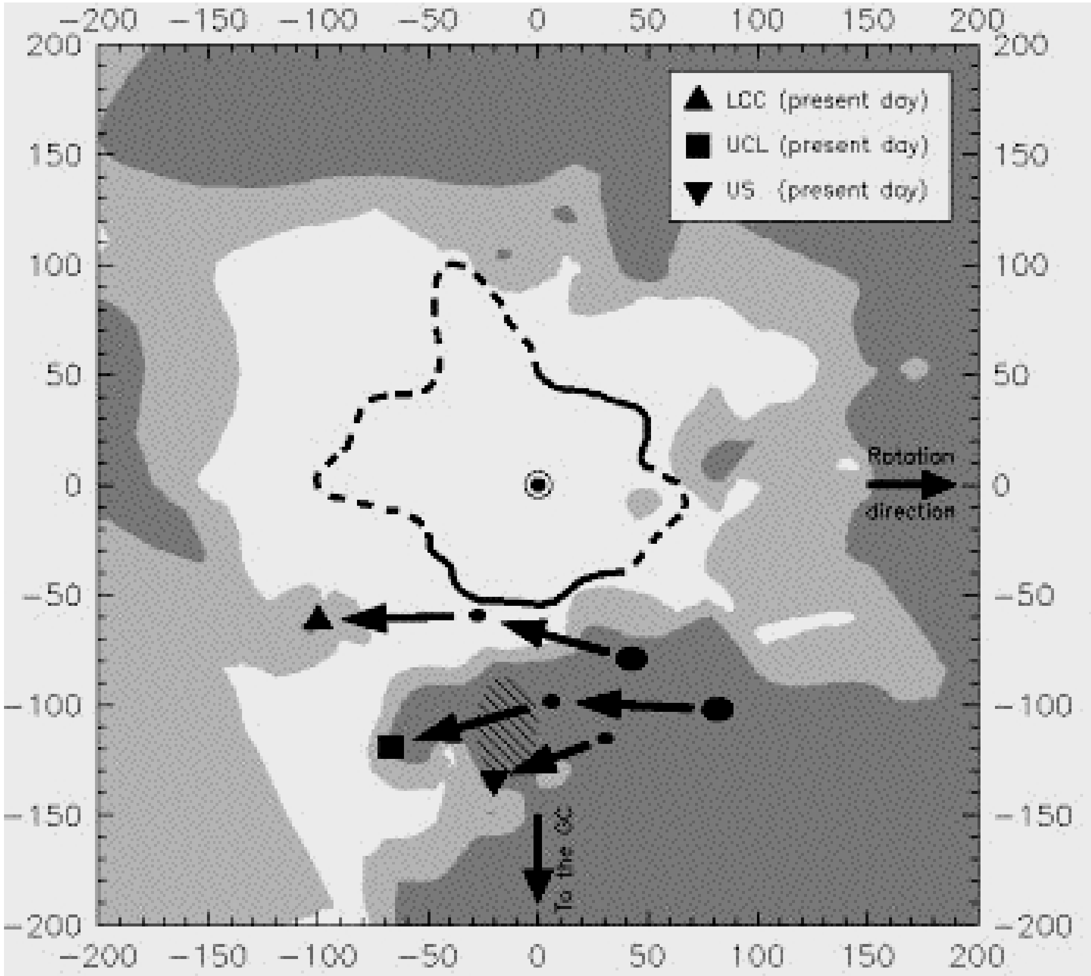

Solar Wind Charge Exchange (SWCX)

- Solar wind ions receive electrons from neutrals
  - O^{7+} + H or He -> O^{6+*} + H^+ or He^+
  - Variation with solar cycle
  - Coronal mass ejections add to intensity
- X-ray emission:
  - Heliospheric contribution >> geocoronal contribution
  - Non isotropic
  - Varies on long and short time scales, can not forecast
  - 1/4 keV: Robertson & Cravens (2003) model explains ~50% of 1/4 keV emission found in Gal. plane and ~25% of emission at high latitudes
  - 3/4 keV (O VII and O VIII) Koutroumpa et al (2007) model can explain all the local O VII and O VIII on MBM 12 and filament sight lines, but with unknown error bars
  - Do not expect O VI intensity or ions

Considering a Diminished Hot LB

- Suppose part (1/2) of the X-rays are SWCX and part (1/2) are hot LB, what are the consequences?
- Weaker hot LB
  - Reduces density by ~ $1/\sqrt{2}$, assuming unchanged LB radius and temperature
    - reduces pressure to more reasonable value
  - Decreases estimated energy of the LB
    - Need less explosion energy -> fewer SNRs
    - Perhaps a single SNR could be viable
  - Could change LB temperature, depending on SWCX spectra
  - O VI column density unaffected
  - Lowers the X-ray to O VI ratio
    - Re-opens the door to the break-out model
    - Evaporating clouds modeling could be unaffected by changes in n_e, T

History: Local Interstellar Cloud

- Known in 1980's (i.e. Frisch & York 1983)
- Size = few parsecs
- T ~ 8000 K -- far cooler than LB
- Expect O VI-rich interface region
  - $N_{OVI} = 0.7$ to $1.4 \times 10^{13}/cm^2$
  - $I_{OVI} \approx 250$ ph/s/cm^2/sr
  - Ref: Slavin 1989
- Local Cloud is one of many clouds within LB (example: 6 on εCMa line of sight, Gry et al 1995)

- (Figs: Schwarzchild 2000, after Colorado group. Cloud flowing past Sun, away from Sco-Cen association)

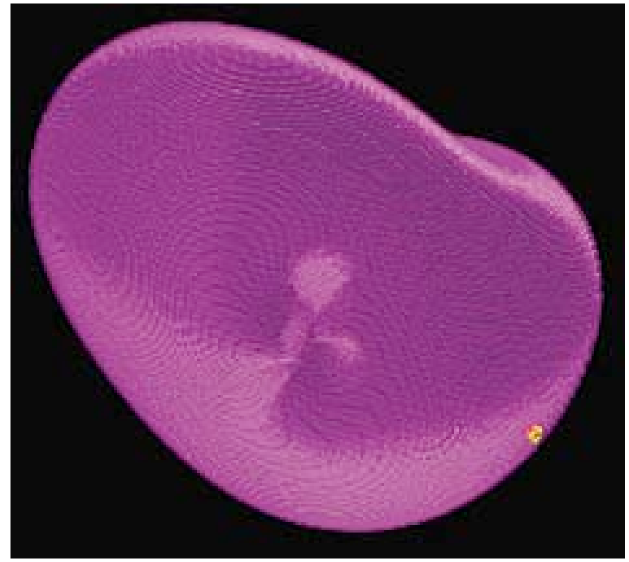

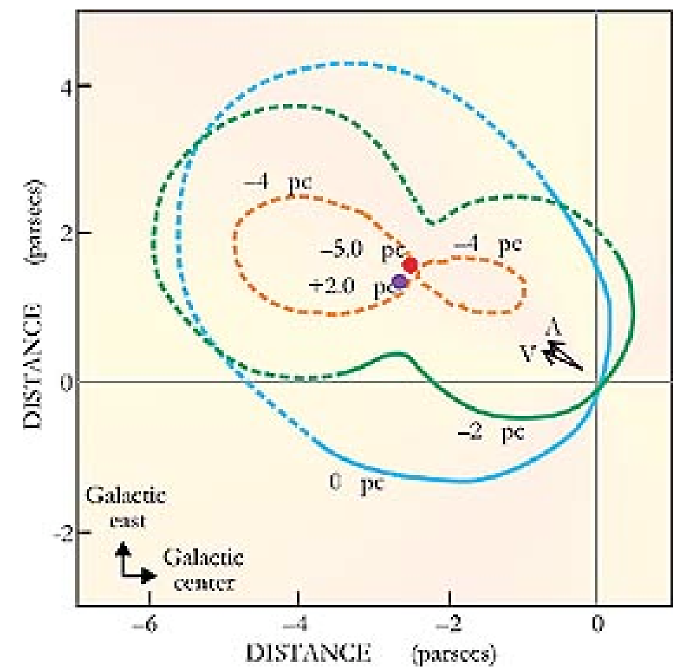

Conclusions

- The Local Bubble may be weaker than previously thought
- This solves some problems (ex: excess pressure)
- It would be difficult to explain all observations if there were no Local Bubble
- However, solar wind charge exchange emission contaminates X-ray observations

1/4 keV X-ray Maps

Left: Soft X-ray Background: Snowden et al. (1997)

Right: 1/4 keV Local component: Snowden et al. (1998)

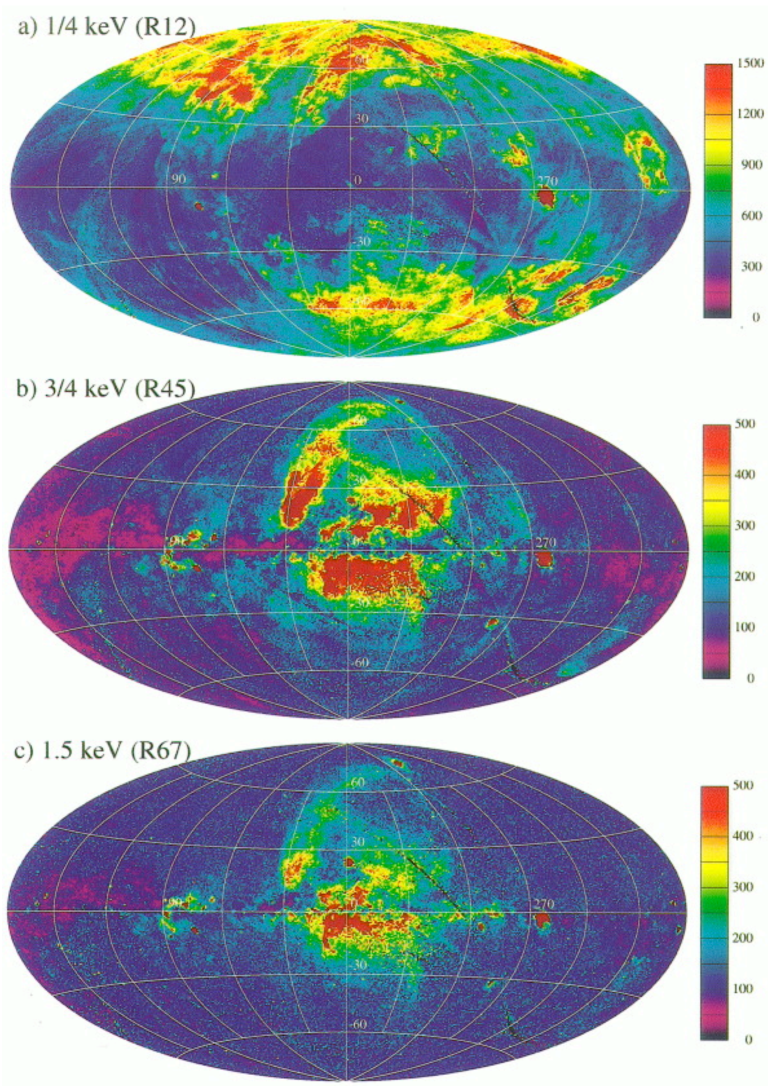

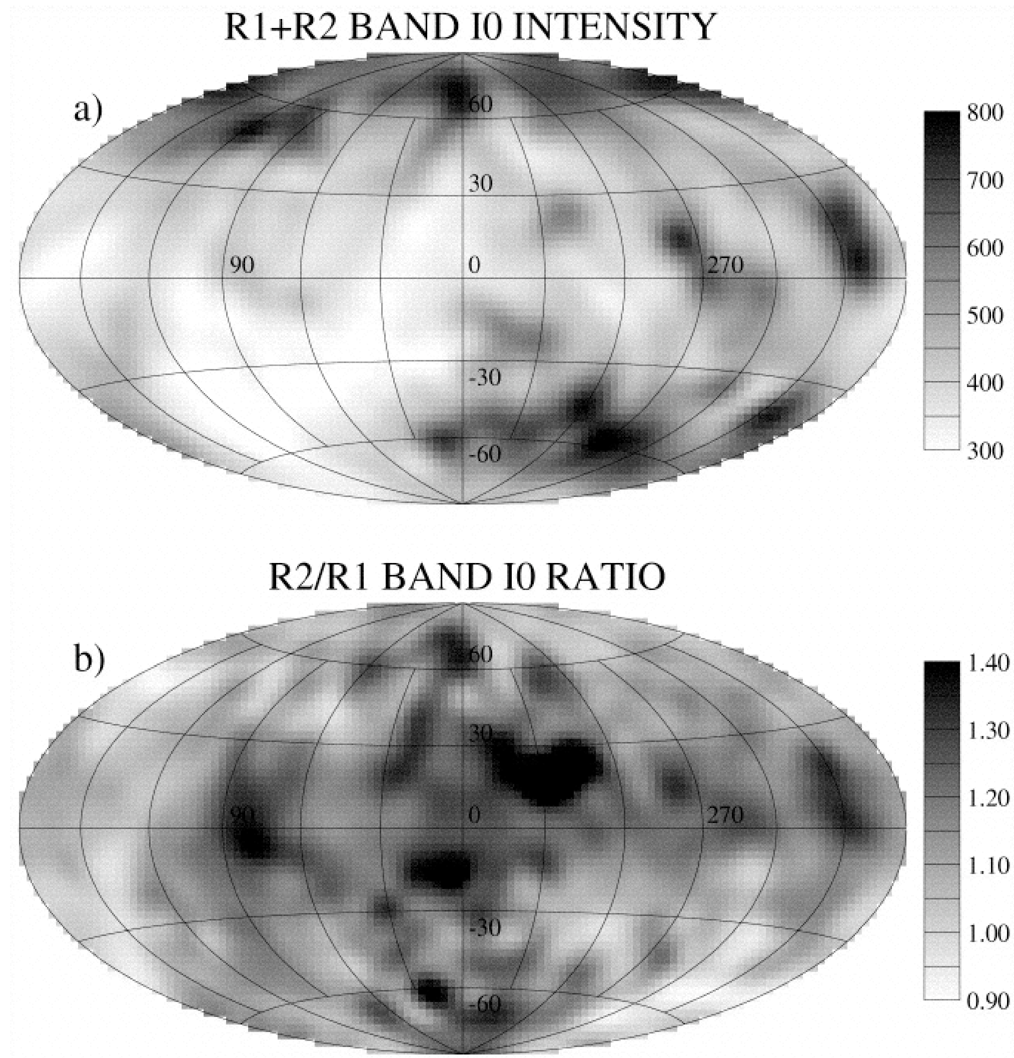

Local O VI Column Densities

TABLE 1

Summary of the Observational Data

WD Name	Other Name	l (deg)	b (deg)	d (pc)	T_{eff} (K)	Type	v_* (km s^{-1})	v_{LISM} (km s^{-1})	References
WD 0004+330	GD 2	112.48	−28.69	97	49360	DA1	NM	+0.1	a, 1
WD 0027−636	MCT 0027−6341	306.98	−53.55	238	63724	DA	(+30.2)	(+0.6)	b, 2
WD 0050−332	GD 659	299.15	−84.12	58	36000	DA1.5	+34.3	+9.8	a, 3
WD 0113+002	HS 0111+0012	134.85	−61.88	...	65000	DO	NM	(−18.1, +33.1)	b, 2
WD 0147+674	GD 421	128.58	+5.44	99	30210	DA	NM	(−9.6)	b, 2
WD 0416+402		160.20	−6.95	228	35227	DA	(+79.1)	(−2.3, +19.6)	a, 2
WD 0455−282	MCT 0455−2812	229.29	−36.17	102	57200	DA1	+69.6	+14.0	a, 1
WD 0549+158	GD 71	192.03	−5.34	49	32750	DA1.5	NM	+23.2	a, 1
WD 0603−483		255.78	−27.36	178	35332	DA:	(+41.0)	(−39.3, +15.3)	a, 2
WD 0715−703		281.62	−23.50	94	43600	DA	NM	(−9.0)	a, 2
WD 0802+413		179.22	+30.94	230	45394	DA	(+58.5)	(+15.3, +70.7)	b, 2
WD 0809−728		285.82	−20.42	121	30585	DA	NM	(−4.1)	c, 2
WD 0830−535		270.11	−8.27	82	30500	DA	NM	(+9.2)	c, 2
WD 0937+505		166.90	+47.12	218	36200	DA	NM	(−5.1)	b, 2
WD 1017−138		255.74	+34.53	90	32000	DA	NM	(−7.5)	a, 2
WD 1041+580	PG 1041+580	150.12	+52.17	93	30800	DA	NM	(−10.1)	a, 2
WD 1100+716		134.48	+42.92	141	43000	DA	NM	(−14.8)	b, 2
WD 1211+332	HZ 21	175.03	+80.02	115 ± 35	53000	DO2	(+14.8)	−18.0	d, e, 2, 1
WD 1234+481		129.81	+69.01	129	56400	DA1	NM	−28.9	a, 1
WD 1254+223	GD 153	317.26	+84.75	67	38686	DA1.5	NM	−5.0	a, 4
WD 1314+293	HZ 43	54.10	+84.16	68 ± 13	50560	DA1	NM	−6.8	f, g, 4
WD 1335+700		117.30	+46.80	104	30289	DA	NM	(−24.5)	b, 2
WD 1440+751	HS 1440+7518	114.10	+40.12	98	42400	DA:	NM	(−18.1)	a, 2
WD 1528+487		78.87	+52.72	140	47600	DA1	(+48.6)	(−85.0, −21.6)	a, 2
WD 1603+432	PG 1603+432	68.23	+47.95	114	35075	DA	NM	(−26.2)	b, 2
WD 1615−154	EGGR 118	358.79	+24.18	55	29732	DA1.5	NM	−38.2	f, h, 1
WD 1620+647		96.61	+40.16	174	30184	DA	NM	(−36.7)	b, 2
WD 1631+781	1ES 1631+78.1	111.29	+33.58	67	44560	DA1+dMe	NM	−11.8	a, 1
WD 1634−573	HD 149499 B	329.88	−7.02	37 ± 3	49500	DO+KOV	+0.6	−19.6	h, i, 5
WD 1636+351		56.98	+41.40	109	37200	DA	NM	(−12.5)	a, 2
WD 1648+407		64.64	+39.60	200	38800	DA:	NM	(−27.2)	a, 2
WD 1800+685		98.73	+29.78	159	46000	DA1	NM	−15.9	a, 1
WD 1844−223		12.50	−9.25	62	31600	DA1	NM	(−41.1)	a, 2
WD 1845+683		98.84	+25.65	125	37400	DA	NM	(−18.1)	a, 2
WD 1917+595	HS 1917+5954	91.02	+20.04	111	33000	DA	(+12.2)	(−24.2)	b, 2
WD 1942+499		83.08	+12.75	104	34400	DA:	(−8.0)	(−36.4)	b, 2
WD 1950−432		356.49	−28.95	140	41339	DA	(+40:)	(−7.5)	b, 2
WD 2000−561	MCT 2000−5611	341.78	−32.25	198	47229	DA	(−15.4)	(−24.2)	b, 2
WD 2004−605		336.58	−32.86	58	44200	DA1	NM	−28.0	a, 1
WD 2014−575	RE J2018−572	340.20	−34.25	51	27700	DA	NM	(−34.4)	c, 2
WD 2111+498	GD 394	91.37	+1.13	50	37360	DA1.5	+28.9	−6.2	a, 1
WD 2116+736	RE J2116+735	109.39	+16.93	177	54680	DA	NM	(−18.0)	b, 2
WD 2124−224		26.81	−43.19	224	49800	DA	+29.5	−14.8	j, 3
WD 2146−433	BPS CS 22951−0067	356.97	−49.44	362	67912	...	(+27.0)	(−7.7)	b, 2
WD 2309+105	GD 246	87.26	−45.11	79	58700	DA1	−12.9	−7.9	a, 1
WD 2321−549	RE J2324−54	326.91	−58.21	192	45860	DA:	(+9.9)	(−11.1)	b, 2

References.—The distance and temperature of the WDs are from (a) Vennes et al. 1997; (b) J. Dupuis et al. 2006, in preparation; (c) Vennes et al. 1997; (d) Perryman et al. 1997; (e) Dreizler & Werner 1996; (f) Finley et al. 1997; (g) van Altena et al. 1995; (h) Napiwotzki et al. 1995; (i) Holberg et al. 1998; (j) Vennes et al. 1998. Distances with errors are from parallax measurements, others are photometric distances. The stellar (v_*) and LISM (v_{LISM}) heliocentric velocities are from (1) *IUE* (Holberg et al. 1998), (2) *FUSE* (this work); (3) *HST*/STIS (Bannister et al. 2003); (4) *HST*/STIS (Redfield & Linksy 2004), (5) *HST*/GHRS (Wood et al. 2002). For *IUE* and *HST* the error on the absolute heliocentic velocity is $\lesssim 3$ km s^{-1}; for *FUSE* the error on the absolute velocity is unknown and the values are therefore listed inside parentheses. "NM" stands for no metal detected in the *FUSE* bandpass.

TABLE 7

LISM O vi and O i Column Densities

WD Name	d (pc)	log N_a(O vi) (cm^{-2})	log N(O i) (cm^{-2})
WD 0004+330	97	12.79 ± 0.09	16.35 ± 0.15
WD 0455−282	102	13.42 ± 0.07	14.91:
WD 0549+158	49	<12.62	$14.27^{+0.07}_{-0.09}$
WD 0715−703	94	13.23 ± 0.07	$15.90^{+0.10}_{-0.09}$
WD 1017−138	90	13.29 ± 0.11	$15.95^{+0.45}_{-0.22}$
WD 1211+332	115	$12.38^{+0.17}_{-0.28}$	15.74 ± 0.05
WD 1234+481	129	12.91 ± 0.08	$15.63^{+0.08}_{-0.07}$
WD 1254+223	67	13.10 ± 0.05	$14.25^{+0.06}_{-0.05}$
WD 1314+293	68	12.94 ± 0.06	14.51 ± 0.03
WD 1528+487	140	13.27 ± 0.06	15.80 ± 0.08
WD 1615−154	55	<12.94	$15.78^{+0.10}_{-0.09}$
WD 1631+781	67	$12.52^{+0.12}_{-0.17}$	15.90 ± 0.09
WD 1634−573	37	13.04 ± 0.06	15.51 ± 0.03
WD 1636+351	109	$12.95^{+0.12}_{-0.20}$	$15.71^{+0.24}_{-0.13}$
WD 1800+685	159	12.96 ± 0.07	$16.12^{+0.14}_{-0.12}$
WD 1844−223	62	<12.84	15.97 ± 0.08
WD 2004−605	58	13.00 ± 0.10	15.65 ± 0.08
WD 2124−224	224	13.07 ± 0.11	15.94 ± 0.03
WD 2309+105	79	<12.53	15.67 ± 0.04

Notes.—The O vi column densities are from the AOD values listed in Table 3 for WDs with no evidence of stellar contamination. The limits are 2 σ. The O i column densities are from Lehner et al. (2003) and references therein, except toward WD 1254+223, which is from Oliveira et al. (2005). See Table 1 for distance references.

- Left: Savage & Lehrner (2006) sample
- Right: Savage & Lehrner O VI detections with no evidence of stellar contamination; this table is the subset that also has O I data.

More O VI Column Densities

TABLE 1

SUMMARY OF TARGETS AND OBSERVATIONS

												O VI RESULTS 1032Å			O VI RESULTS 1038Å		
HD	NAME	SPECTRAL TYPE	l	b	R(pc)	V	E(B-V)	v SIN i	v STAR	v INT	v GALACTIC ROTATION	LOG N	$\bar{v}$	$\langle(v-\bar{v})^2\rangle$	LOG N	$\bar{v}$	$\langle(v-\bar{v})^2\rangle$
5394	γ Cas	B0.5 IVe1	123.6	-2.1	213	2.6	0.08	300	0.1	3.4	-3.4	<12.00	...	...	<12.30	...	...
10144	α Eri	B3 Vp	290.8	-58.8	26	0.5	0.04	411	5.0	...	-0.1	13.06[10]	6.9	453	----	J & M	----
14633	HD 14633	ON8 V	140.8	-18.2	2061	7.5	0.10	126	-36.6	-3.9	-34.1	13.72	-11.2	565	<13.60	...	...
22928	δ Per	B5 III	150.3	-5.8	78	3.0	0.04	271	-11.0	4.2	-1.1	<13.70	...	...	----	J & M	----
23630	η Tau	B7 III	166.7	-23.5	57	2.9	0.03	216	-3.8	7.8	-0.4	<13.30	...	...	----	J & M	----
24398	ζ Per	B1 Ib	162.3	-16.7	377	2.9	0.33	72	13.6	6.3	-3.5	13.18	13.5	299	----	J & M	----
24760	ε Per	B0.5 III	157.4	-10.1	316	2.9	0.10	150	-3.9	3.2	-3.8	12.94	57.6	260	----	J & M	----
24912	ξ Per	O7.5 III (n) ((f))	160.4	-13.1	542	4.0	0.32	216	64.1	5.1	-5.7	13.34	1.2	299	----	J & M	----
28497	HD 28497	B1.5 Ve2	208.8	-37.4	445	5.6	0.02	340	-5.6	...	5.1	13.86[12]	-7.9	639	---	York (1974)	---
30614	α Cam	O9.5 Ia	144.1	14.0	1164	4.3	0.32	95	8.7	-3.4	-18.6	<13.40	...	...	----	J & M	----
33328	λ Eri	B2 IVn	209.1	-26.7	263	4.3	0.05	336	-15.1	-13.0	3.4	13.65	-11.0	655	13.26	-10.8	352
35439	25 Ori	B1 Vn	201.0	-18.3	315	4.9	0.05	316	2.6	5.0	3.4	12.98	3.3	131	13.13	-14.4	172
36486	δ Ori A	O9.5 II SB	203.9	-17.7	429[4]	2.2	0.07	148	-1.2	8.1	5.1	13.74	-20.5	1570	----	J & M	----
36695	HD 36695	B1 V SB	204.8	-17.8	398	5.4	0.06	183	4.9	9.5	4.9	13.92[10]	-10.1	487	13.84	-3.0	273
36861	λ Ori A	O8 III ((f))	195.1	-12.0	573	3.5	0.12	75	18.3	10.1	4.8	13.21	-7.9	701	----	J & M	----
37043	ι Ori	O9 III SB	209.5	-19.6	470	2.8	0.07	122	5.4	-8.9	6.5	13.30	-18.9	351	----	J & M	----
37128	ε Ori	B0 Ia	205.2	-17.2	492	1.7	0.08	85	8.7	7.7	6.2	13.17	-6.0	131	13.27	-9.6	146
37303	HD 37303	B1.5 V	209.8	-19.1	547	6.0	0.02	260	10.7	8.0	7.6	13.55	-23.7	322	13.66	-23.2	370
37742	ζ Ori A	O9.7 Ib IB	206.5	-16.6	404	1.9[9]	0.09	127	0.6	6.0	5.2	13.25	-1.6	279	----	J & M	----
38666	μ Col	O9.5 V	237.3	-27.1	701	5.2	0.01	108	87.1	-4.9	10.1	13.82	1.1	1061	---	York (1974)	---
38771	κ Ori	B0.5 Ia	214.5	-18.5	597	2.1	0.07	81	1.9	1.8	9.0	13.40	-5.8	432	----	J & M	----
40111	139 Tau	B1 Ib	184.0	0.8	1191	4.8	0.15	131	-3.2	2.4	2.8	13.83	5.8	376	----	J & M	----
41161	HD 41161	O8 Vn	165.0	12.9	1202	6.5	0.17	300	0.9	6.9	-10.0	13.29	17.4	63	...	...	...
42933	δ Pic	B0.5 IV SB	263.3	-27.7	766	4.8	0.04	270	12.5	-4.1	3.6	13.59	-18.4	555	13.71	-18.9	810
44506	HD 44506	B1.5 IIIn	241.6	-20.8	817	5.5	0.05	211	34.7	...	11.6	13.84	0.9	787	13.87	-1.5	903
45995	HD 45995	B2.5 Ve2+	200.6	0.7	340	6.1	0.12	320	-34.9	7.8	3.8	13.29	16.2	344	13.34	16.6	187
47839	15 Mon	O7 V((f))	202.9	2.2	705	4.6	0.07	106	18.0	7.7	8.6	13.50	22.1	670	----	J & M	----
51283	HD 51283	B2 III	234.0	-9.3	485	5.3	0.05	248	18.5	...	7.9	13.78	12.9	546[11]	...	...	...
52918	HD 52918	B1 IV	218.0	0.6	459	5.0	0.06	336	7.3	6.6	7.6	13.09	46.6	202	13.10	51.2	410
57060	29 CMa	O7 Ia:fp SB	237.8	-5.4	2228[5]	4.9	0.17	136	-5.7	8.6	38.9	13.46	16.6	570	----	J & M	----
57061	τ CMa	O9 II SB	238.2	-5.5	933	4.4	0.15	120	21.7	8.2	15.0	13.52	15.4	508	----	J & M	----
58978	HD 58978	B0.5 IVnpe1	237.4	-3.0	776	5.6	0.16	244	29.1	...	12.6	13.97	30.0	499	13.86	23.3	376
64740	HD 64740	B1.5 Vp	263.4	-11.2	281	4.6	0.03	274	-9.7	...	1.2	13.25	8.2	543[11]	13.06	-15.6	425
64760	HD 64760	B0.5 Ib	262.1	-10.4	973	4.2	0.10	259	23.2	...	6.2	14.08[10]	14.6	709[12]	14.13	15.0	665
66811	ζ Pup	O4 I(n) f	256.0	-4.7	433[6]	2.3	0.06	185	-42.0	-16.0	3.8	13.51	0.7	544	----	J & M	----
68273	γ^2 Vel	WC8 + O9 I	262.8	-7.7	382[7]	1.8	0.04	...	-35.5	-5.0	1.9	13.65	-11.6	328	----	J & M	----
87901	α Leo	B7 V	226.4	48.9	22	1.3	0.01	354	-2.9	...	0.2	<13.40	...	...	----	J & M	----
91316	ρ Leo	B1 Iab	234.9	52.8	1052	3.8	0.08	69	36.7	13.7	10.8	13.20	-15.6	413	----	J & M	----
93521	HD 93521	O9 Vp[1]	183.1	62.2	1507	6.9	0.10	303	-14.6	-9.0	1.3	13.86[10]	-14.1	529	13.94	-20.0	894
104337	HD104337	B1 V SB	286.9	41.6	423	5.3	0.05	138	-2.2	-10.0	-2.7	13.18	-15.6	224	13.60	-3.1	236
106490	δ Cru	B2 IV	298.2	3.8	145	2.8	0.0	218	11.8	...	-2.0	12.72	49.9	199	12.92	53.9	142
112244	HD112244	O8.5 Iab(f)	303.6	6.0	1472	5.4	0.34	138	15.4	-18.4	-20.1	13.86	-19.3	393	...	...	...
116658	α Vir	B1 IV SB	316.1	50.8	84[8]	1.0	0.03	196	4.5	-6.0	-0.9	13.43[10]	5.4	180	---	York (1974)	---
120307	ν Cen	B2 IV SB	314.4	19.9	189	3.4	0.01	94	7.9	...	-3.0	13.17	18.5	507[12]	13.53	16.4	645
120315	η Uma	B3 V	100.7	65.3	41	1.8	0.02	216	1.5	...	-0.1	<12.40	...	...	----	J & M	----
121263	ζ Cen	B2.5 IV SB	314.1	14.2	110	2.5	-0.02	191	4.5	...	-1.8	13.10	-3.1	258	13.20	-15.6	239
121743	φ Cen	B2 IV	316.0	19.1	225	3.8	0.02	115	4.1	...	-3.6	12.71	-8.6	58	13.15	-4.0	181
122451	β Cen A	B2 III IB	311.8	1.3	126	0.6	0.02	161	-13.1	...	-2.1	12.96	13.8	260	---	York (1974)	---
132058	β Lup	B2 III	326.3	13.9	153	2.7	0.02	130	3.0	...	-2.3	13.28	6.5	692	13.58	1.0	435
135591	HD135591	O7.5 III ((f))	320.1	-2.6	1169	5.4	0.23	131	1.6	-0.4	-18.7	13.62	5.1	469	13.54	9.1	505
136298	δ Lup	B1.5 IV	331.3	13.8	212	3.2	0.03	235	4.0	...	-2.9	13.34	-3.2	263	13.19	-9.8	160
143018	π Sco	B1 V + B2	347.2	20.2	196	2.9	0.08	100	5.6	-6.3	-1.3	12.40	-4.3	299	----	J & M	----
143118	η Lup A	B2.5 IV	338.8	11.0	129	3.4	-0.01	242	6.4	...	-1.4	13.21	-9.9	280	13.41	-9.4	404
143275	δ Sco	B0.5 IV IB	350.1	22.5	186	2.3	0.16	174	6.3	-2.3	-1.0	13.26	-2.6	113	----	J & M	----
149881	HD149881	B0.5 III[2]	31.4	36.2	1690	6.6	0.12	...	31.0	1.7	19.7	13.54	12.2	194[11]	<13.48	...	...
150898	HD150898	B0.5 Ia	330.0	-8.5	2547	5.6	0.18	108	-56.2	-2.0	-34.8	13.84	-4.8	415	13.42	8.7	396
151890	μ^1 Sco	B1.5 IV SB	346.1	3.9	245	3.0	0.05	216	-18.3	...	-1.9	13.44	-13.0	343[12]	13.28	-10.9	149
155806	HD155806	O7.5 V(n)e	352.6	2.9	745	5.5	0.32	211	-14.3	3.9	-3.2	14.22[10]	-5.1	568	14.03	-8.9	182
157246	γ Ara	B1 Ib	334.6	-11.5	658	3.3	0.08	353	-4.3	-5.9	-8.4	13.16	-5.1	351	----	J & M	----
158926	λ Sco	B1.5 IV IB	351.7	-2.2	144	1.6	0.03	237	4.7	6.6	-0.7	13.26	-13.0	260	---	York (1974)	---
165024	θ Ara	B2 Ib	343.3	-13.8	755	3.7	0.09	139	6.9	...	-6.8	...	...	...[13]	13.63	-17.8	286
173948	λ Pav	B2 II-III	333.6	-23.9	404	4.2	0.09	217	14.0	2.1	-4.9	13.78[10]	17.0	690	13.56	-11.7	472
175191	σ Sgr	B3 IV IB	9.6	-12.4	72	2.1	0.0	213	-0.6	-13.0	0.4	<12.90	...	...	----	J & M	----
180968	2 Vul	B1 IV	56.4	4.9	413	5.4	0.28	332	20.1	5.6	6.2	14.10[10]	23.1	1006	...	...	...
184915	κ Aql	B0.5 IIIn	31.8	-13.3	646	5.0	0.27	276	-4.0	28.3	9.4	13.57	18.6	280	...	...	...
186994	HD186994	B0.2 IV[3]	78.6	10.1	2089	7.3	0.0	126	...	...	5.3	14.00	10.1	93[11]	<13.85	...	...
200120	59 Cyg	B1.5 Ve2nn	88.0	1.0	245	4.8	0.18	450	16.9	-5.0	0.2	13.12	2.5	99	----	J & M	----
200310	60 Cyg	B1 Vn	87.2	0.1	384	5.4	0.06	320	5.9	1.5	0.4	13.16	14.1	206	13.27	-23.3	340
209952	α Gru	B7 IV	350.0	-52.5	30	1.7	-0.02	290	10.0	...	-0.1	<12.87	...	...	---	York (1974)	---
214080	HD214080	B1 Ib[1]	44.8	-56.9	3236	6.7	0.05	102	3.6	8.6	24.7	13.46	22.3	93[14]	<13.49	...	...
214168	8 Lac A	B1 Ve1	96.4	-16.1	413	5.7	0.12	348	0.6	-0.5	-1.8	13.55	-9.1	401	13.84	-4.3	783
219188	HD219188	B0.5 II-III(n)[3]	83.0	-50.2	2228	6.9	0.12	185	52.9	-2.7	-0.3	14.10[10]	-6.2	808[12]	<13.48	...	...

1 Numerous references cited in Jaschek, et al. (1964).

2 Lesh and Aizenman (1975).

3 Walborn (1973).

4 Δm = 1.5 from Cester (1965).

5 Δm = 1.0 from Seyfert (1941).

6 M_v = -6.1 from Morton (1976).

7 M_v = -6.0 from Hanbury Brown, et al. (1970).

8 From Herbison-Evans, et al. (1971).

9 Value of 1.77 in Lesh (1968) refers to components A and B together.

10 P(N, 1.05 × 10^{13} cm^{-2}, $m_s r_0$) <0.025, see § IVb of Paper II.

11 The tracing of the other HD feature at 1021 Å is of poor quality. Hence the correction for HD absorption is uncertain.

12 The scans for HD at 1021 Å were not recorded, because of satellite malfunctions.

13 HD absorption seen at 1021 Å is so large that reliable subtraction at 1032 Å cannot be performed with presently available data.

14 Virtually no flux from the star was seen at 1021 Å. Hence no correction for HD was made.

- Jenkins (1978) *Copernicus* survey

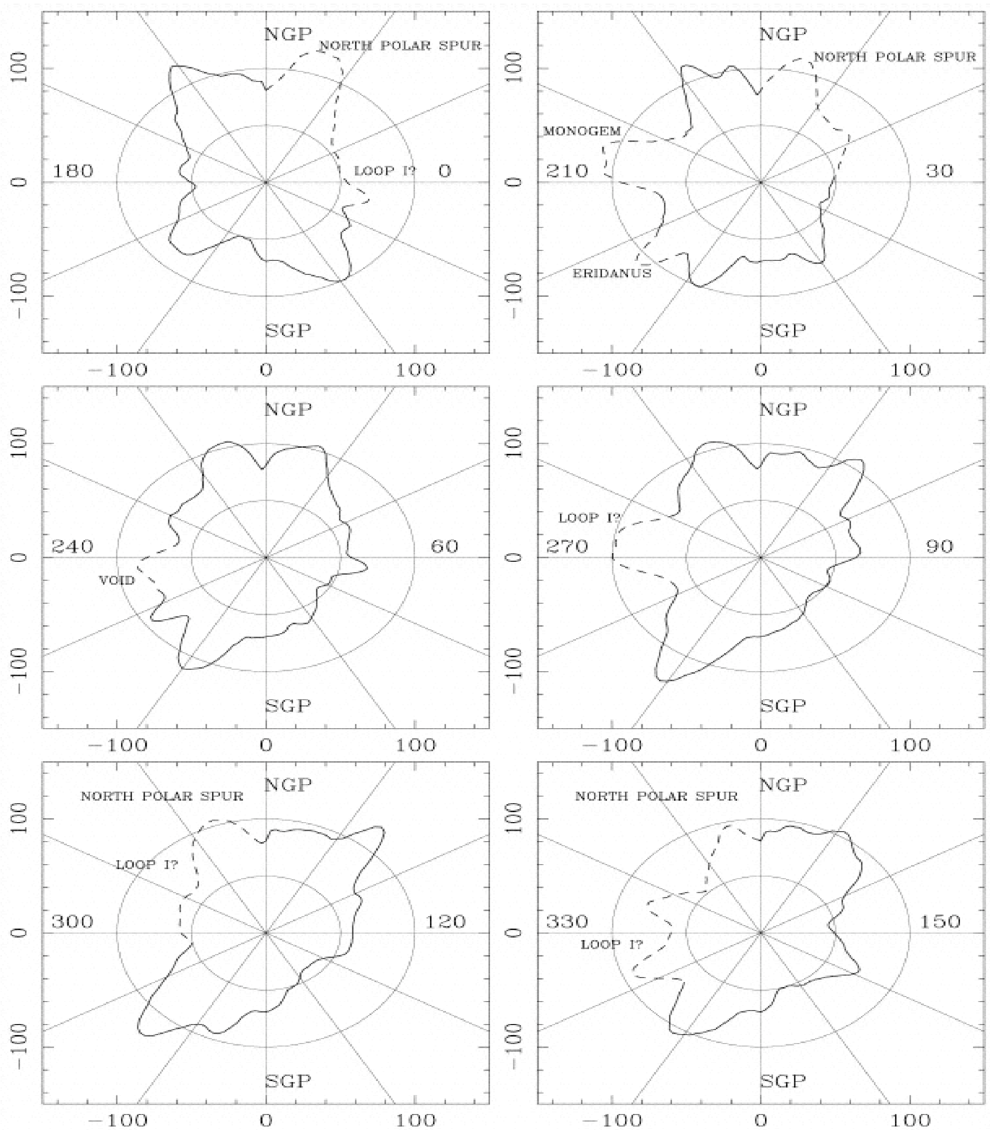

Snowden et al. 1998

More supplemental slides

Why Should We Care?

- If there is no hot gas in the LB, and little other gas, then we have an unexplained hole (the Local Cavity) in the Galaxy
  - (hole should fill in at the speed of sound in the surrounding medium, which should be observable, also local clouds should expand at this speed, which should be observable)
- If the LB does exist, then it is our local example of the population of hot bubbles in galaxies

Before the Local Bubble (was known)

- Early 1970's: *Copernicus* UV observations
  - Interstellar O VI absorption (Jenkins & Meloy 1974, Jenkins 1978a)
- Jenkins 1978b developed spatial model
  - Based on column density fluctuations
  - Regions of O VI-rich gas distributed in Galaxy
- O VI traces ~3 x 10^5 K (assuming collisional ionizational equilibrium (CIE))

  ∴Hot gas regions distributed within Galaxy

The Local Bubble Emerges

- Local (r < 100 pc) region emits soft (~1/4 keV) X-rays
- Name ➡ Local (Hot) Bubble
- Temperature: if CIE, then $T \sim 10^6$ K, $P \sim 15{,}000$ K/cm^3
- Obs sources: Wisconsin All Sky Survey, SAS 3, HEAO 1, ROSAT, (XMM, Chandra)

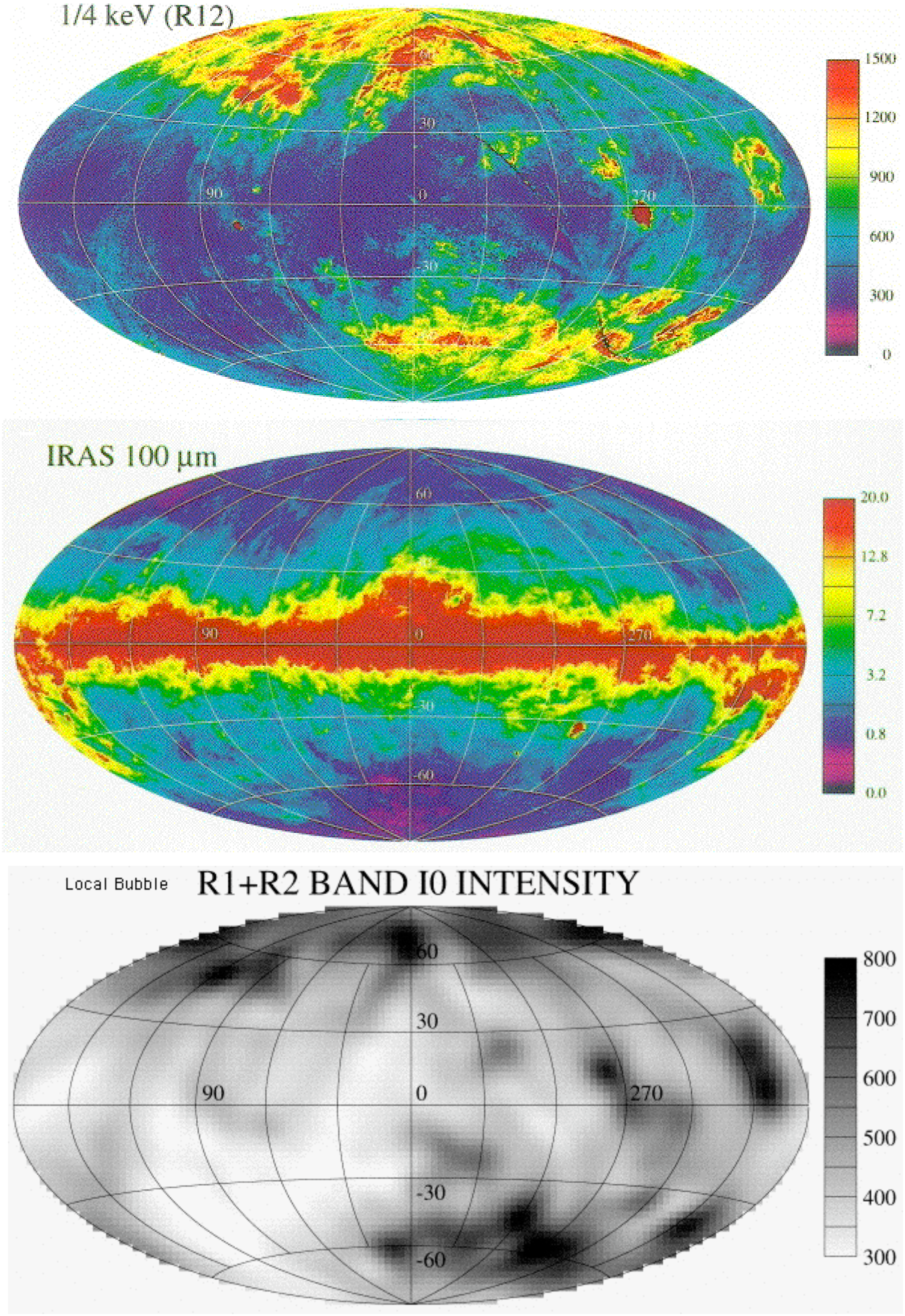

Figures from Snowden et al. 1997, 1998

Cartoon Geography:

Local Cavity,

Local Bubble,

and

Embedded Clouds

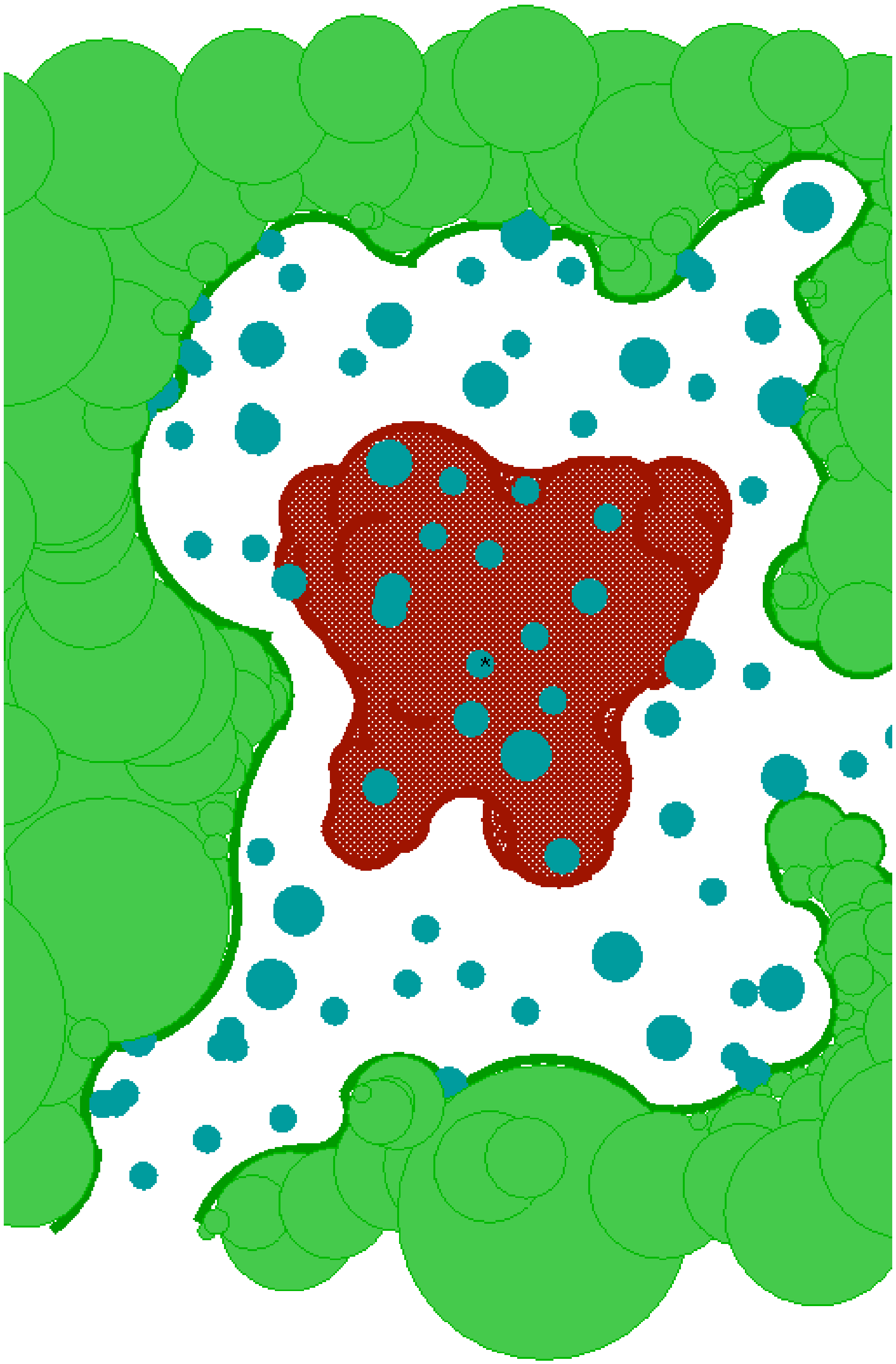

Copernicus Revisited

- Jenkins' O VI spatial model revised to include LB (Shelton & Cox 1994)

- $N_{LB} \approx 1.6 \times 10^{13}$ cm^2

  (attributed to bubble boundary + interface with Local Cloud)

- Also, $N_{\text{distant features}}$ ➡ larger than in Jenkins 1978b

Recent Observations: O VI Emission

- FUSE shadowing observation ➡ isolate Local Bubble intensity
- Tight Upper Limit:

  $I_{OVI(2\sigma)} \leq$ 800 ph/s/cm^2/sr
- Much less than expected from "breakout" model
- Tightly constrains bubble and evaporating clouds models
  - minimal number of cloud boundaries, minimal emission per cloud boundary, and very dim Local Bubble
- Ref: Shelton 2003

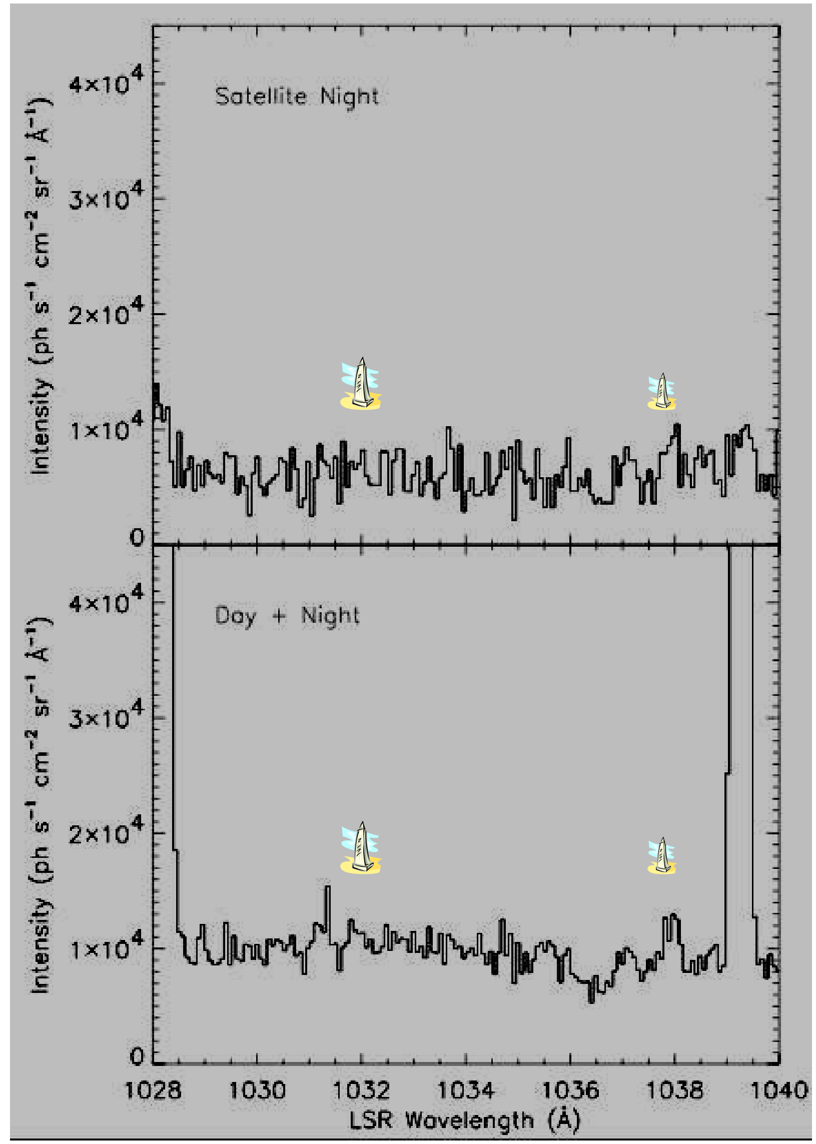

New Column Densities

- FUSE Local ISM Survey:
  N_{LB} ($r \le 100$ pc) $\approx 7 \times 10^{12}/cm^2$
- Too little O VI for "breakout" model
- See O VI within LB ➡ interpreted as transition zones on clouds
- Hard to see a wall of O VI at LB boundary ➡ problem for hot bubble models
- Ref: Oegerle, Jenkins, Shelton, Bowen & Chayer, submitted
- GI Obs: Welsh et al. 2002
  ($N_{OVI} < 10^{13}$ cm^2, d = 120 pc, high lat)

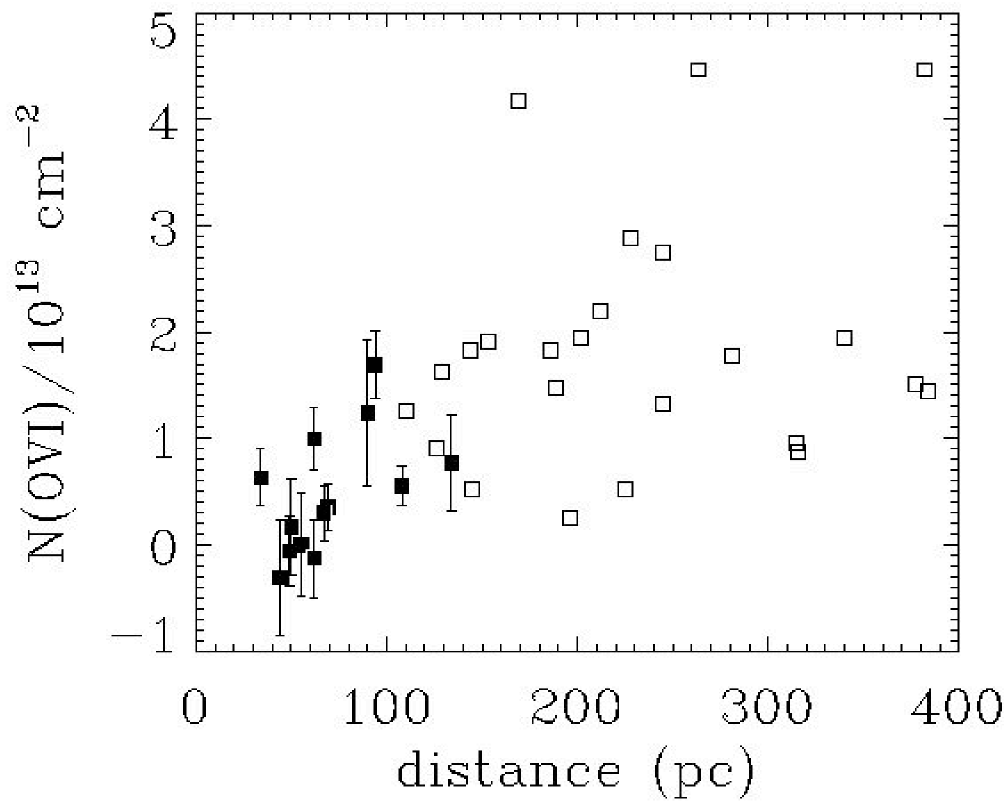

Discussion

☐ What We Don’t See:

- Not enough O VI ions or resonance line photons for the “breakout” model
- Don’t see strong LB boundary ➡ this isn’t your standard theoretical bubble
- Dim emission constrains net bubble + clouds model

☑ What We Do See:

- O VI ions inside the LB ➡ possibly cloud boundaries, lots of them, but wimpy
- LB region has more O VI than average ISM ➡ “rumors of the LB’s demise have been greatly exaggerated”

Power Law Emission Measure Models

- $d(n_e^2 dl)/dT \propto T^\beta$
- 2 versions:
- Yao & Wang (2007) modeled O VI (abs), O VII & O VIII (abs + emiss) together, Mrk 421 and l ~ 90°, b~61°
  - Found $\beta = 0.6$
- Lei, Shelton, & Henley (in preparation), used O VI (abs & emiss), ROSAT 1/4 keV, and Suzaku spectrum (covered O VII & O VIII) from Southern Filament shadowing analysis (l = 279°, b=-47°)
  - Required 2 components
  - Found β_1= -0.6, and β_2 = -3

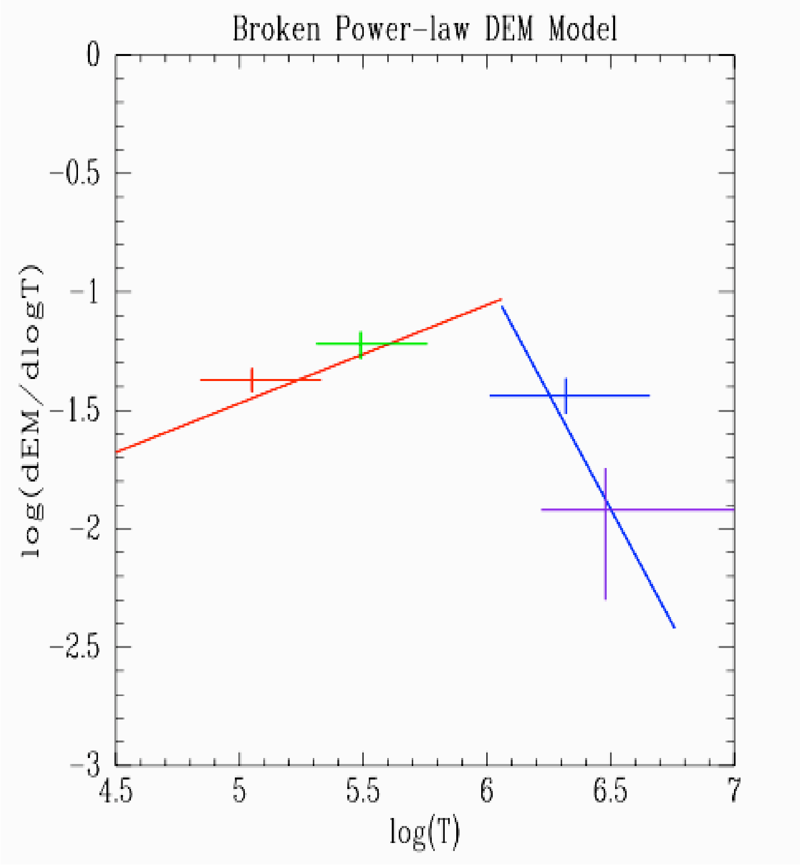

Sources of hot gas:

SNRs (other talks)
Superbubbles
Possibly Pervasive Gas
Halo
Alert: solar wind contamination

NGC 4631 Galaxy. credit: NASA, CXC, HST, UIT, GSFC, AURA, NSF, D. Wang et al.

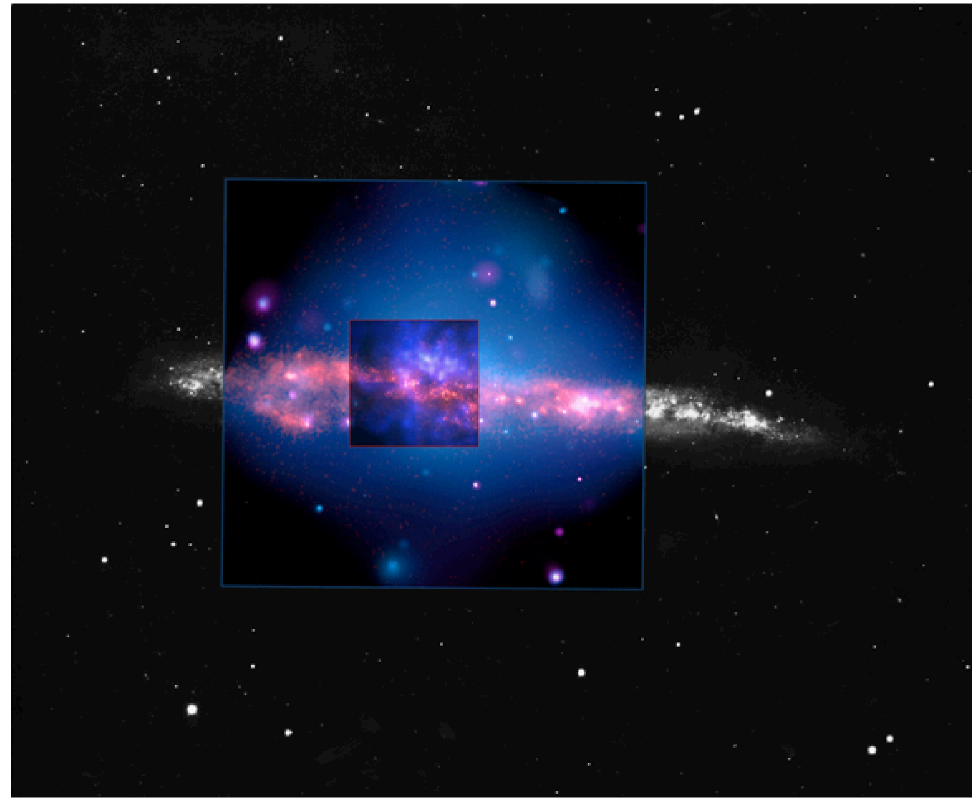

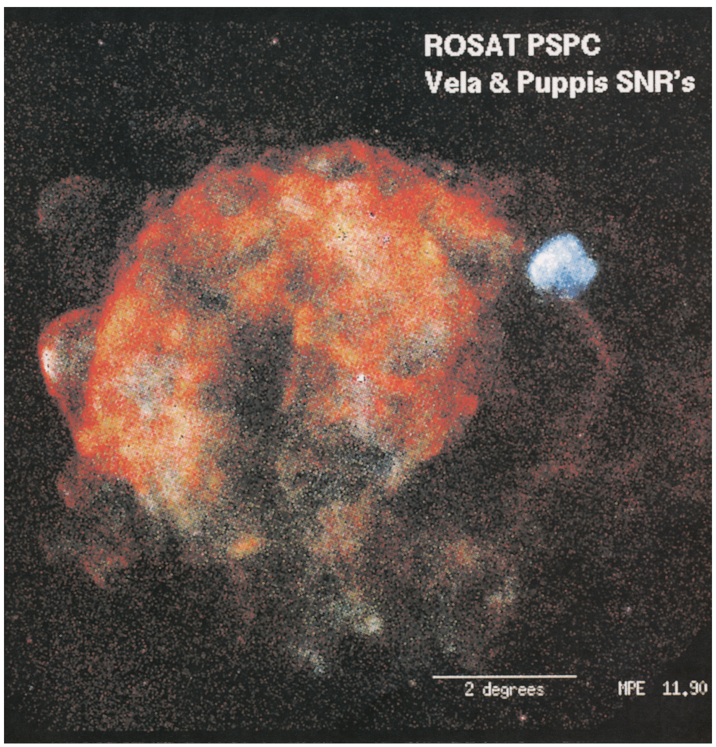

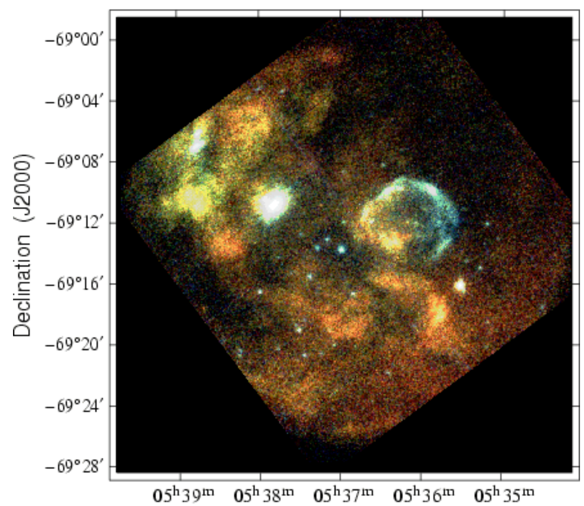

Dennerl, et al. 2001   Right Ascension (J2000)
X–Ray Image from XMM (very hot gas)

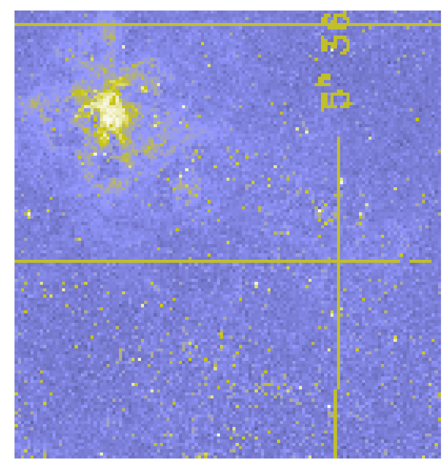

Visible (DSS)

How Can We Make Progress on SWCX?

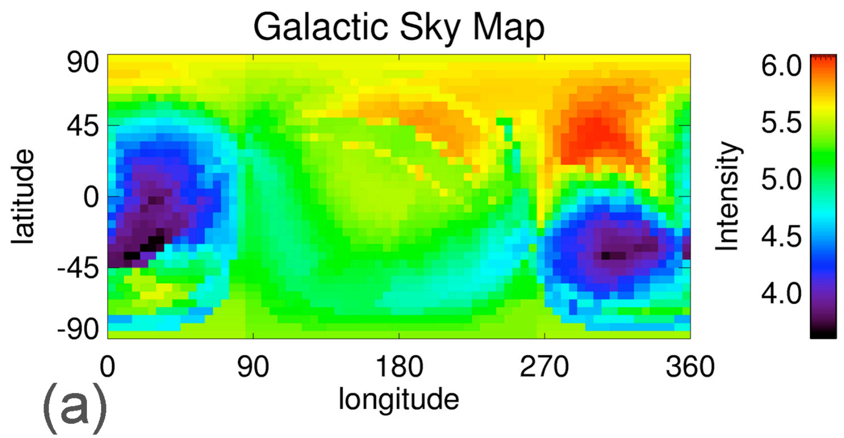

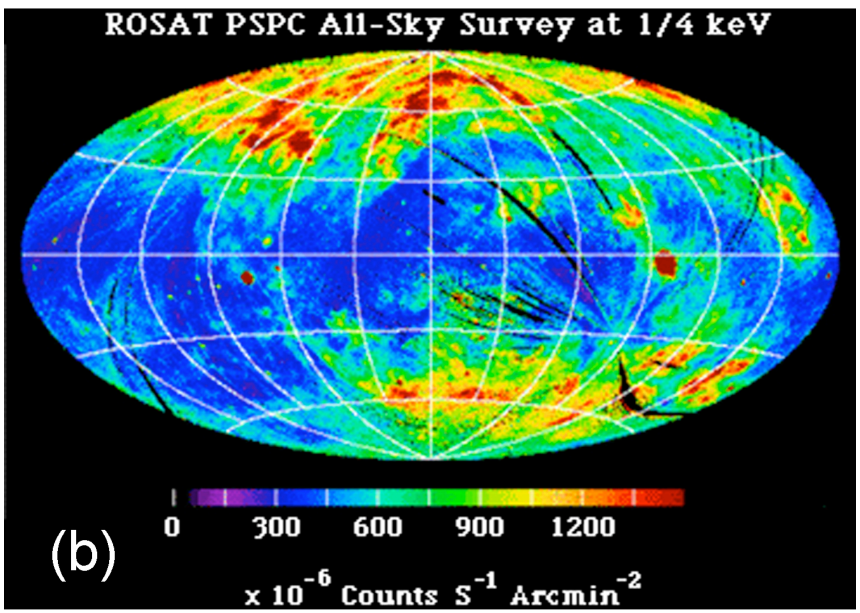

- Continue work on SWCX estimates
  - improved atomic physics in the 1/4 keV band
  - uncertainty estimates
  - spectral temperature of the SWCX and remaining LB spectra
- Search for LB by making additional X-ray shadowing observations in directions with dim SWCX and bright local emission (i.e. high ecliptic latitude, high positive galactic latitude)

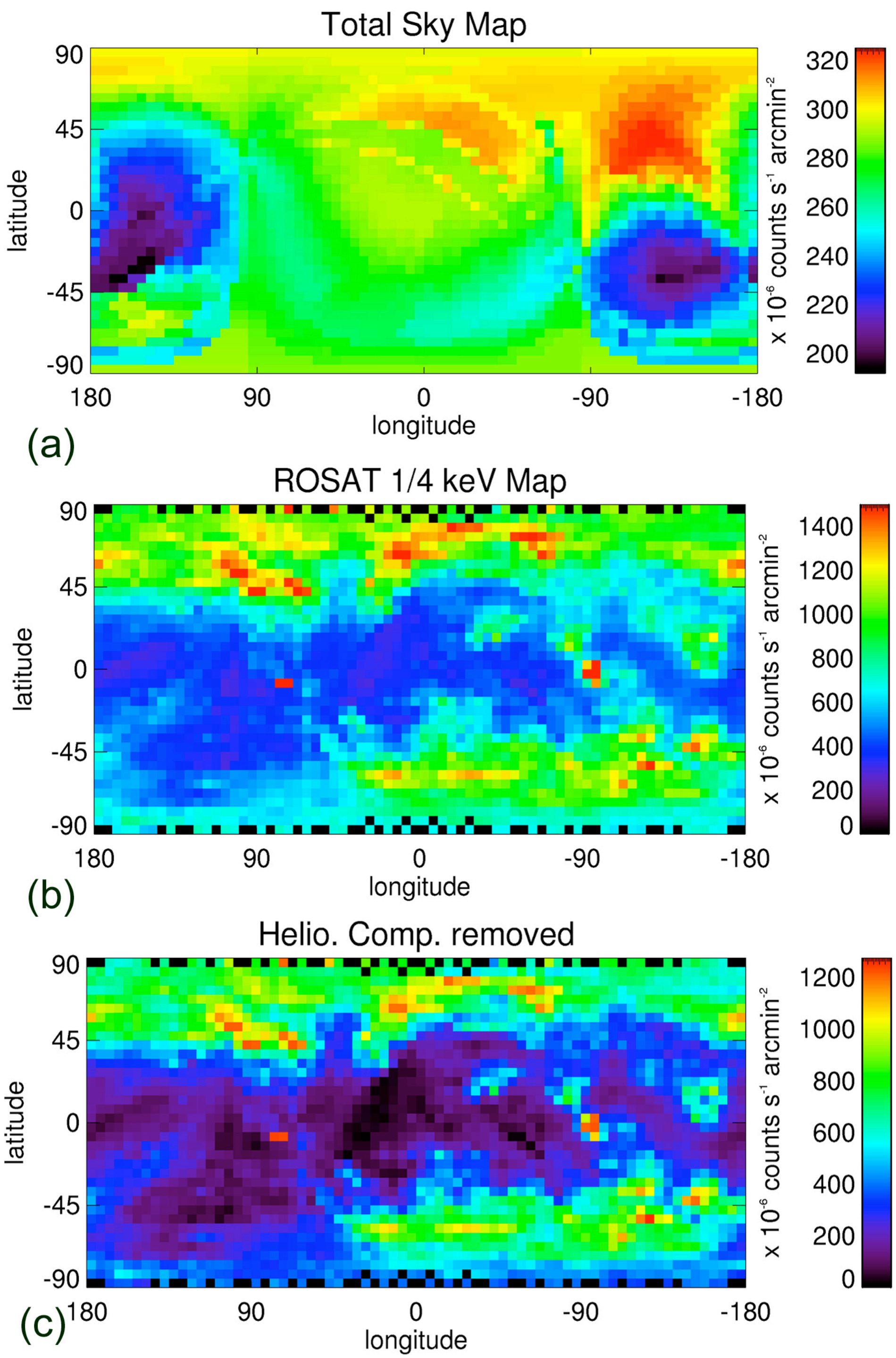

Predicted Heliospheric X-Ray Emission as seen From Earth.
-- in galactic coordinates.

Robertson, Cravens, and Snowden (2003).

ROSAT SXRB
Map is also shown and an approximate "subtraction" map.

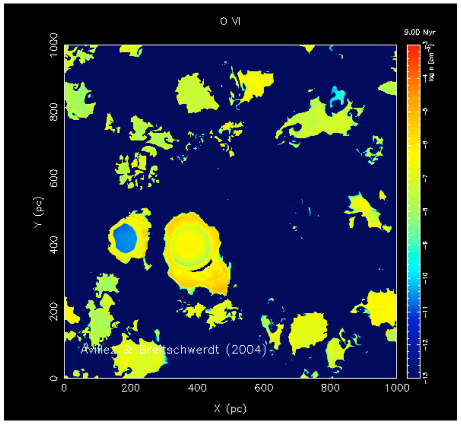
O VI
9.00 Myr
Avillez & Breitschwerdt (2004)
X (pc)
Y (pc)

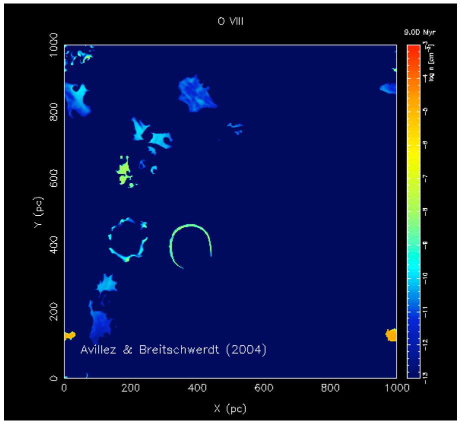
O VIII
9.00 Myr
Avillez & Breitschwerdt (2004)
X (pc)
Y (pc)

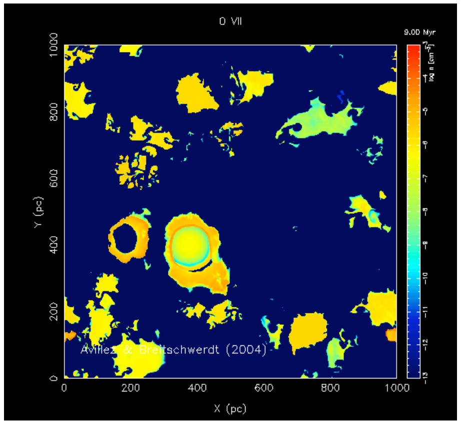
O VII
9.00 Myr
Avillez & Breitschwerdt (2004)
X (pc)
Y (pc)